Synthesis of $Ni_{0.5}Zn_{0.5}Fe_2O_4$/MWCNT Nano- hybrid by Ultra- Sonication Assisted Method for Enhanced Dielectric Properties

By

Shahbaz Ali

School of Chemical and Materials Engineering (SCME)

National University of Sciences and Technology

(NUST)

2017

Synthesis of $Ni_{0.5}Zn_{0.5}Fe_2O_4$/MWCNT Nano- hybrid by Ultra- Sonication Assisted Method for Enhanced Dielectric Properties

Name: Shahbaz Ali

Reg. No: NUST201362309MSCME67713F

This thesis is submitted as a partial fulfillment of the requirements for the degree of

MS (Materials & Surface Engineering)

Supervisor Name: Dr. Iftikhar Hussain Gul

School of Chemical and Materials Engineering (SCME)

National University of Sciences and Technology (NUST), H-12

Islamabad, Pakistan

September, 2017

Certificate

This is to certify that work in this dissertation has been carried out by **Mr. Shahbaz Ali**. He completed his project under my supervision in Thermal Transport Laboratory, School of Chemical and Materials engineering, National University of Sciences and Technology, H-12, Islamabad, Pakistan.

Supervisor**: Dr. Iftikhar Hussain Gul**
Department of Materials Engineering
School of Chemical & Materials
Engineering,
National University of Sciences and
Technology, Islamabad

Submitted through:

Principal**: Prof. Dr. Arshad Hussain**
Department of Materials Engineering,
School of Chemical & Materials
Engineering,
National University of Sciences and
Technology, Islamabad-Pakistan

Dedication

I dedicate this thesis to my beloved family for their dedicated love and support leading me to success in life.

Acknowledgements

All praise to Allah the most beneficial. I feel honored to acknowledge my research supervisor Dr. Iftikhar Hussain Gul to who has pushed me on to complete my work, without his help I would have not attained this level of understanding and commitment. Without his unrelenting efforts, it might have had not been possible for me to complete this task in time.
My sincere regards to our Lab Attendants Mr. Shams, Mr. Khurram and Mr. Shams who helped me in their full capacity. Finally, I wish to offer a humble gratitude to my family for their advice and insight in every aspect life which helped me create my own path in life.

It's all thanks to this affection, love and prayers I received from the above mentioned people that I have reached so far in my life.

Sincerely
Shahbaz Ali

Abstract

Composite Nickel- Zinc ferrites nanoparticles have been developed using co-precipitation technique with the chemical formula of $Ni_{0.5}Zn_{0.5}Fe_2O_4$. A nanohybrid is achieved by coating MWCNTs with ferrites using xylene as a dispersive medium. Different loadings of the MWCNTs have been applied to see the effect of CNTs on the crystal structure and dielectric properties. The loadings applied were 0%, 1%, 2%, 3% and 5%. X-Ray Diffraction and Scanning Electron Microscopy techniques have been applied to ensure the structure and morphology of the nanohybrid which measure the crystal size to be in the range of 25nm to 50 nm. Dielectric measurements have been made which show dramatically increased performance at low frequency ranges due to the addition of MWCNTs. The highest values of dielectric constant achieved were $3.29x10^4$, while the highest value of dielectric loss was $4.35x10^5$. These values were achieved for the most loading of MWCNTs, i.e. 5% XRD patterns show no characteristic peak of MWCNTs meaning that the CNTs have been completely decorated by the ferrite nanoparticles. The SEM images further confirm this result. The method proved to be efficient for the coating ferrites using xylene as a dispersive medium and improving dielectric properties and should be further investigated using polymer matrix to further enhance the dielectric loss allowing it to be used in the application of microwave absorption.

Table of Contents

List of Figures

List of Tables

Chapter: 1

Introduction

1. Spinel Ferrites:

Spinel Ferrites also known as Ceramic Ferromagnetic Nano- materials have been considered the most important Electronic Materials for over a century. In these prolonged years, the commercial quality of both soft and hard ferrites are reaching optimum theoretical values[1]. Various methods may be used to obtain ultrafine powders of Nano-ferrites classified into two categories namely, Solid State Methods and Wet Chemical Methods E.g. Hydrothermal, Co-precipitation, Sol-Gel etc. Among these two categories, Wet Chemical Methods are usually preferred over Solid State Methods due to the less energy required as of low sintering temperatures acceptable levels of homogeneity achieved, and a relatively smaller particle size.

1.1 Brief History

The terminology "Magnetism" was derived from "Magnesia", an island of Aegean Sea which was home to a certain types of minerals, named lodestones, had the property of attracting iron were discovered in 470 B.C. Magnets were employed in various navigation applications by Chinese back in the 13^{th} Century. In the mid of 16^{th}century, William Gilbert, a famous physicist, manufactured synthetic magnets by stroking iron chunks with lodestones and proved that the compass will consistently point towards north because earth, having a rotating molten iron core, possesses magnetic properties. In 1750, John Michell stated the magnetic poles fulfil the **Inverse Square Law**, further established via Charles Coulomb. After the discovery; a magnetic field is produced by an electric current, the first electromagnet was manufactured in 1825. Later, Faraday, Bergmann and Becquerel discussed the effect of magnetism on liquids and gases, noticeable responses were found only in a few. Currently, magnets are used everywhere ranging from simple household equipment to applications on massive industrial scales. To understand the concept of magnetism, the whole center revolves around the dipole and magnetic field perspectives, the term "**Magnetic Field**" describes the space where

energy has changed. This variation of energy within the space may easily be observed and calculated. The "**Magnetic Poles**" may be thought of a point where the magnetic field detected is either entering or leaving the magnetic material. Magnetic poles may never exist in isolation, instead they occur as two poles of opposite nature with some distance between them, forming a dipole e.g. a bar magnet having two poles, a north (magnetic field is leaving the material) and a south (magnetic field is entering the material). Two dipoles or magnets can be created bar magnet is cut in half, this may continue up to the scale of atoms. Hence, magnetism may originate from the basic building block. A material's property to respond to magnetic field applied is known as magnetism. Some materials are attracted by the magnetic fields while some are repelled, and some are unaffected. There are two important quantities which relate B (magnetic flux density) and M (magnetization) to H (magnetizing force). The magnetic susceptibility 'χ' and the magnetic permeability 'μ', defined below:

$$\chi = M / H \qquad (1.1)$$

$$\mu = B/H \qquad (1.2)$$

1.1.1 Source of Magnetism:

Everything in this universe in made up of atoms which, in turn, are made up of protons, electrons and neutrons. Protons and neutrons are present in the nucleus while electrons revolve around the nucleus. Electrons carry a negative charge, and it is this movement of the charge that produces a magnetic field. The strength of said field is known as magnetic moment. Let's consider an electronic current moving through a conductor, as electrons are flowing, a magnetic field is created all covering this conductor. Such a field may be quantified by movement of the needle in the compass. This movement is due to a force being experienced on this needle, acknowledging the existence of a dipole. All matter is affected by this magnetic field and each material responds as of its nature.

1.2 Classification of Magnetic Materials:

Upon the placement of a material within a magnetic field, the material can react, depending upon various factors including the molecular and atomic level of the structure or the net magnetic moments inhabited by the individual atoms. The magnetic moments of an electron in an atom are associated with the electron's orbital motion and spinning motion, both are affected by the applied magnetic field. Some materials align parallel to the applied field while others align opposite to it[1].

In atoms, electrons are usually present in pairs, spinning in opposite directions which causes their net magnetic field to be zero. Materials with unpaired electrons possess net magnetic field. Based upon these characteristics, a material's behavior may be classified as:

1. Diamagnetism
2. Paramagnetism
3. Ferro/Ferrimagnetism
4. Antiferromagnetism
5. Superparamagnetism

1.2.1 Diamagnetism:

Diamagnetism is an inherent result of the orbital motion of the electrons in a magnetic field. Present in materials with zero net magnetic moment. The orbital motion generates a field opposite to the applied field (magnetization is directed opposite to the applied field, as illustrated in Fig1.1), described by a negative susceptibility. These materials tend to move toward regions of weaker field.

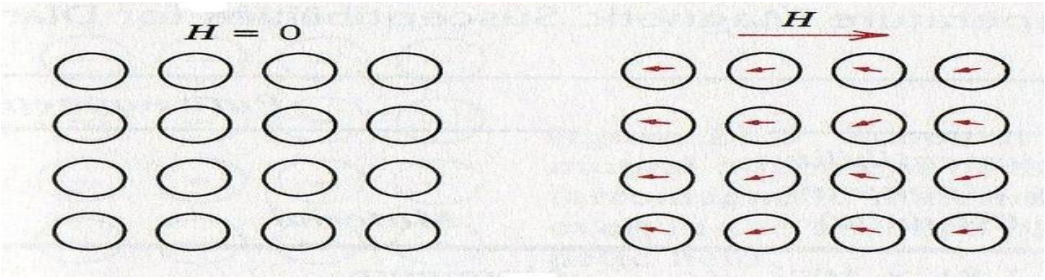

Fig 1.1 Atomic dipole configuration for a diamagnetic material

1.2.2 Paramagnetism:

The partial termination of electron spins/orbital's magnetic moments causing permanent dipole moment leads to Paramagnetic behavior[2]. There is no net magnetization on domain scale when no magnetic field is present i.e. the dipoles are oriented randomly in the domains cancelling each other out. Upon the applying the magnetic field, moments align themselves by rotation, towards the field direction, thus acquiring a net magnetization.

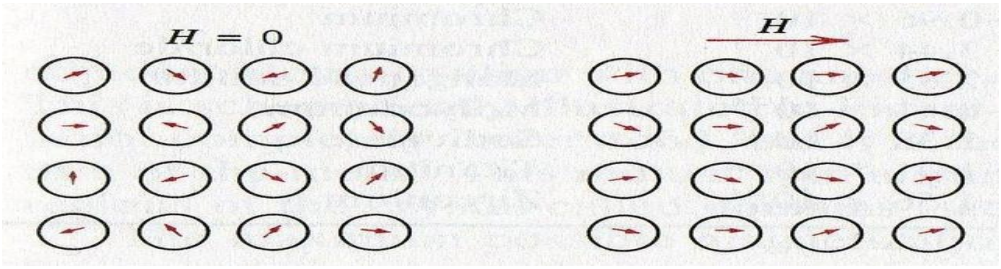

Fig 1.2 Atomic dipole configuration for a paramagnetic material

1.2.3 Ferromagnetism and Ferrimagnetism:

Ferro and ferrimagnetic materials possess a permanent magnetic moment in the absence of an external field and a very large permanent magnetization. In ferromagnetic materials, this permanent magnetic moment is the result of the cooperative interaction of a large number of atomic spins called domains (regions where all spins are aligned in the same direction).

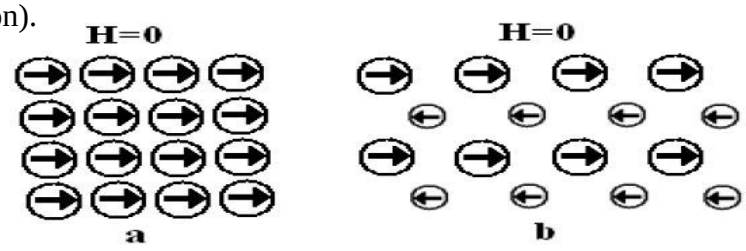

Fig 1.3 Dipole configuration for Ferromagnetic and Ferrimagnetic behavior

In Ferrimagnetic materials, incomplete cancellation of the magnetic dipoles in a domain results in a lower magnetization (Fig 1.3). The macroscopic magnetization of ferro- and ferri-materials is the sum of the magnetizations of the domains which make up the material[3]. Ferrimagnets are ionic solids meaning they are electrically insulating, whereas most Ferromagnets are metals (conductors).”

1.2.4 Anti- Ferromagnetism:

Anti-ferromagnetic behavior consists of magnetic moments associated with the atoms or molecule, related to the electron spin, are usually aligned regularly with the adjacent spins oriented in the opposite direction. Such a behavior exists at very low temperatures, diminishing above a specific temperature known as **Neel Temperature[4]**.

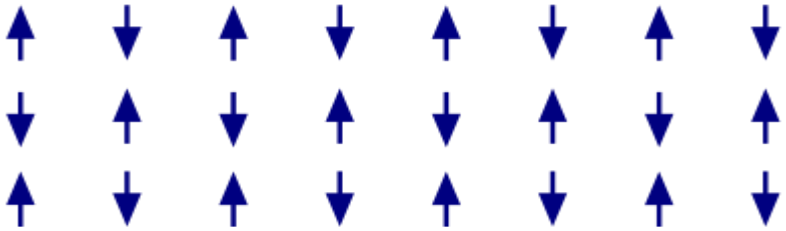

Fig 1.4 Anti-ferromagnetism ordering of dipoles

1.2.5 Superparamagnetism:

A material exhibiting magnetic behavior similar to that of a paramagnetic material when heated below curie temperature or Neel temperature may be called Super Paramagnetic material. Usually, the coupling forces said to exist in a magnetic material causes magnetic moments of adjacent atoms to align with each other, resulting in extensive internal magnetic fields[5].

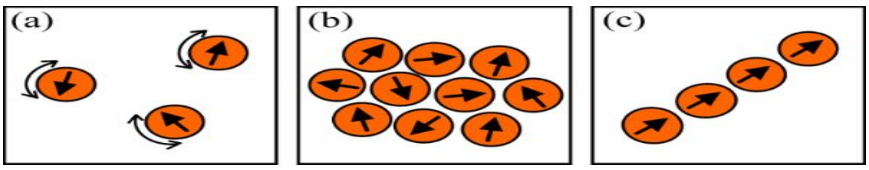

Fig 1.5 Superparamagnetism ordering of dipoles

1.3 Ferrites:

Ferrites are the most important ferrimagnetic materials. Iron oxide (Fe_2O_3) is the principal component in the ferrites. Due to presence of ferrimagnetic oxides, ferrites are insulating materials. Ferrites are magnetic materials which are used to make transformer cores, permanent magnets and are used in many other applications. As they are electrically insulating materials and are highly resistive. They are mostly used in the high frequency application because of their ability to restrict the production of eddy currents. There are two structural symmetries of ferrites based upon the charge and mass of the metal ions. One is the cubical while the other is a hexagonal structure. There are two types of ferrites based on the hysteresis losses.

1.3.1 Soft Ferrites:

Ferrites having low ‘coercivity’ are known as soft ferrites. The ability to dissipate energy while magnetizing or demagnetizing is known as ‘coercivity’ [1]. They usually appear to be black or gray and are very hard and brittle. Soft ferrites have high value of resistivity which is used to prevent the energy losses in the central cores of transformers and inductors. Manganese zinc ferrite and nickel zinc ferrite are the examples of soft ferrites.

1.3.2 Hard Ferrites:

Hard ferrites also called ceramic magnets have a high value of coercivity, meaning the material takes time to demagnetize. The magnetic permeability of the hard ferrites is very high. Hard ferrites are made of iron, strontium and barium oxides and are economically cheap as the raw material is easily available to make hard ferrites. They are used excessively in household appliances due to their low cost. Some of the important hard ferrites are ferrite, strontium ferrite and nickel zinc ferrite [1]. The two types of ferrites are compared in the table given below.

Table 1.1 Comparison between hard and soft ferrites

Soft magnetic Hard magnetic	Hard magnetic Hard magnetic
Low Saturation Magnetization	**High saturation magnetization**
Low Coercivity (Hc)	**High Coercivity (Hc)**
Low Permeability	**High Permeability**
Low Remanence	**High Remanence**
Low Magnetostriction	**High Magnetostriction**
Low Curie temperature (Tc)	**High Curie temperature (Tc)**

1.4 Types of Ferrites:

There are three types of ferrites classified by their structure. We categories ferrites as shown below:

1.4.1 Spinal ferrites

1.4.2 Garnet ferrites

1.4.3 Hexagonal ferrites

1.4.1 Spinel Ferrites:

Spinel ferrites have the general formula MFe_2O_4, where 'M' is a divalent cation. Cobalt (Co^{+2}), Copper (Cu^{+2}), Zinc (Zn^{+2}) and Nickel (Ni^{+2}) are the examples of divalent cations. Spinel ferrites possess a relatively simple structure as compared to the other types of ferrites. The unit cell of the spinel lattice is composed of 32 Oxygen ions. The anions are arranged in a close-packed face centered cubic structure. There are two types of space sites between the anions, referred as A and B sites:

(A). Tetrahedral sites

(B). Octahedral sites

Tetrahedral site is the site which is surrounded by the 4 oxygen atoms. A spinel structure acquires 64 tetrahedral sites. The cations occupy 8 of the tetrahedral sites out of 64. Octahedral site is surrounded by the 6 oxygen atoms. There are 32 octahedral sites in the

spinal ferrite structure. 16 octahedral sites are occupied by anions. The occupation of the A and B sites result into the electrically neutral structure of spinal ferrite.

Consider the cations being spread over two probable locations, three combinations may be achieved: the "normal," the "inverse," and the "mixed" spinel structure. Ni–Zn ferrites with many crystals within a grain, have an inverse spinel structure. The said formation is produced by close packed face centered cubic (FCC) array of anions. The empty holes are filled with cations, but not at all the sites, and is denoted by the formula $(Zn_xFe_{1-x})(Ni_{1-x}Fe_{1+x})O_4$, in which Ni^{2+} ions in B (octahedral) sites, Zn^{2+} ions locate in A interstitial (tetrahedral) sites [3], and Fe^{3+} ions in the spinel lattice involve both tetrahedral A and octahedral B sites.

Table 1.2 shows radii of some common metal ions used in the spinel ferrites [1].

Table 1.2 Radii of some common metal ions used in the spinel ferrites

Ion	Ionic radius Å
Fe^{2+}	0.83
Fe^{3+}	0.67
Co^{2+}	0.82
Zn^{2+}	0.74
Ni^{2+}	0.78
Mn^{3+}	0.70

1.4.1.1 Types of Spinel Ferrites:

Two types of Spinel structure are there:

(a) Normal spinel

(b) Inverse spinel

Normal spinel ferrites consist of trivalent metal ions occupying the B sites while the divalent metal ions occupy the A sites in the crystal structure.

In the case of inverse spinel ferrites crystal structure, the trivalent ions inhabit equally the A and B sites and all divalent metal ions occupy the B sites [1].

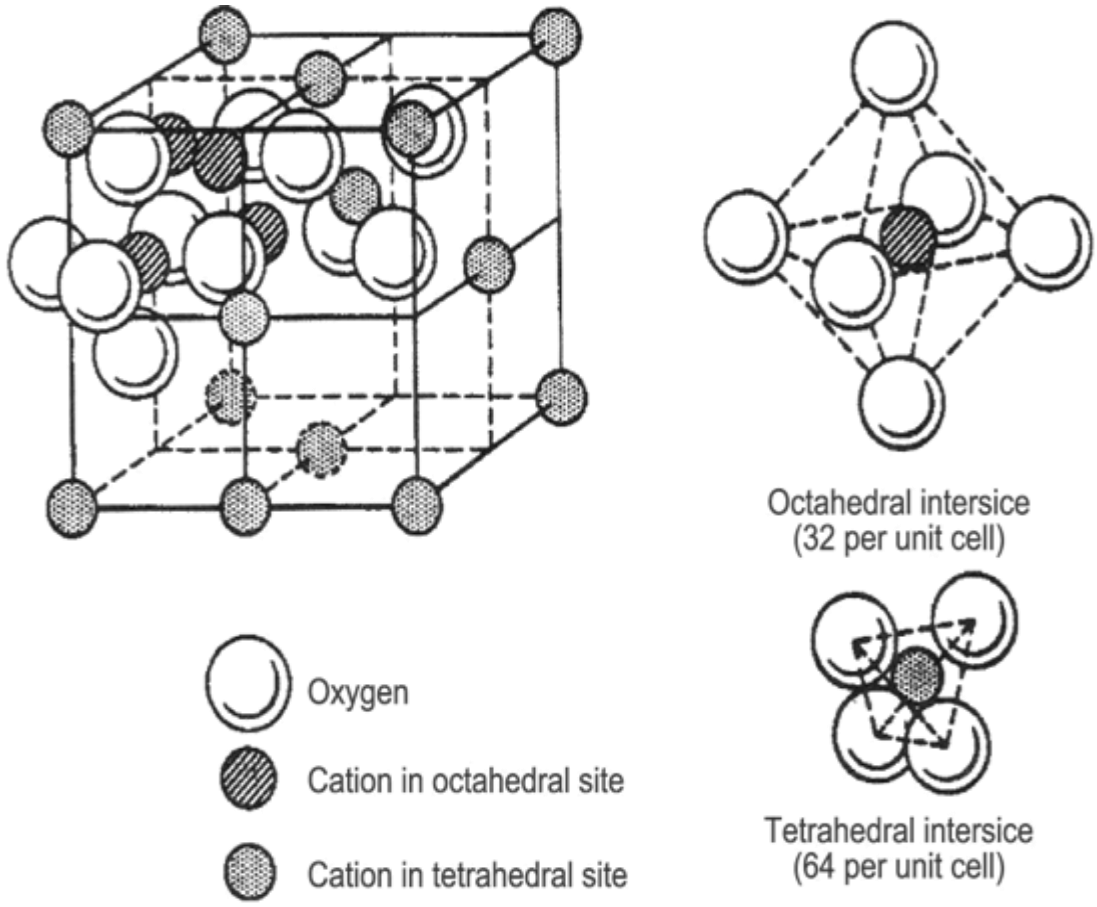

Fig 1.6 Spinel ferrite unit cell with octahedral and tetrahedral sites

(Adopted from: Materials Science and Engineering: An Introduction, 7th Edition, Chapter 20: Magnetic Properties)

1.4.2 Garnet Ferrites:

Giller and Gilleo discover the Garnet ferrites in 1957. Having cubic structure with the general formula $M_3Fe_5O_{12}$ (where M is the rare earth trivalent ion e.g. Y, Gd, and Dy), Garnet ferrites are magnetically hard materials.

1.4.3 Hexagonal Ferrites:

Hexagonal ferrites have the general formula $MFe_{12}O_{19}$. Here M may be nickel, zinc, strontium, barium or a combination of these. Hexagonal ferrites have a high value of coercivity and may be used as permanent magnets [1]. The Hexagonal ferrite structure is alike the spinal ferrite structure. The metal ions occupy the octahedral, tetrahedral and trigonal sites in the arrangment. These magnetic materials are widely used in every field ranging from magnetic recording devices, loud speakers, microwaves to refrigeration magnets. A brief overview of different crystal structure of ferrites including examples are shown below:

Table 1.3 Different types of ferrites

Type	Structure	General Formula	Example
Spinel	Cubic	$M^{II}Fe_2O_4$	M^{II}=Fe, Cd, Co, Mg, Ni and Zn
Garnet	Cubic	$M^{III}_3Fe_2O_{12}$	M^{III}=Y, Sm, Eu, Gd, Tb, and Lu
Magnetoplumbite	Hexagonal	$M^{II}Fe_{12}O_{19}$	M^{II}=Ba, Sr

1.5 Nickel- Zinc Ferrites:

Nickel- Zinc ferrite is a very important material. It has captured the attention of the researchers due to so many useful applications in magnetic fluids, magnetic recording devices, high resistivity and many more. Due to various advances in the field of nanotechnology, many previously thought stale properties have now become subject to revitalized attention in the scientific world. One such property is magnetism which has a vast field of research awaiting it in the nano- scopic scale. Like any property of a solid, the magnetic properties are also dependent upon the microstructure of the material which may be controlled in the processing of the said material. The magnetic properties of a solid material change by the changing the grain size of the material. As we go from the nanometer scale from the micrometer scale, we see a change from the multi- domain to a single domain configuration. This change in the domain size, in turn causes the magnetization process to transfer from domain wall motion as favored in the micron scale to the mechanism of magnetization rotation, which is prominent in single domain. This shift in the magnetization process may cause the overall coercivity of the material to increase. This leads researchers to believe that in order to obtain the optimal performances for soft magnetic materials, the grain size has to be as large as possible. Researchers have also shown that the average grain size of a material is much smaller than a single domain causing the domains the align randomly, in turn having the effect of decreasing the magneto crystalline anisotropy. The result is a massive decrease in coercivity and a massive increase in permeability. As stated above the magnetic behavior of a material is controlled by its microstructure which is controlled by the processing parameters. Thus, to acquire the required magnetic properties of a material without sacrificing the other characteristics one must invest heavily in the processing parameters. Nickel- Zinc ferrite ($Ni_{0.5}Zn_{0.5}Fe_2O_4$) has good chemical stability and excellent mechanical hardness. Nickel- Zinc ferrites are the cubic ferrites. These have the spinal structure. Where Fe^{+3} is located at A and B sites and Ni^{+2} and Zn^{2+} is located at B site. The use of the Nickel- Zinc ferrite in the magnetic recording devices must possess the high value of coercivity. High value of coercivity depends on the particle size of the material. The particle size near the critical size of the particle has the larger value of coercivity. The critical size is equal to the size of single domain. Co-

precipitation and Sol-gel processes are widely used for the synthesis of Nickel- Zinc ferrite nanoparticles. Researchers have found that $Ni_{0.5}Zn_{0.5}$ ferrites have low magnetic coercivity, large permeability, high electrical resistivity and low eddy current loss. Like all properties of a solid, these properties are dependant upon the composition, and ultimately the microstructure of the material, which may be controlled by the processing and the post processing, namely, heat treatment. Recently, Ni- Zn ferrite powders have garnered much attention and various techniques have been used to process ultra- fine samples. Blaskov in (1996) produced the nickel zinc ferrite by using co-precipitation of Iron and nickel zinc solutions. The calcination at 598 K was performed. The nickel zinc ferrite particles with diameter 50 ± 5Å produced. XRD patterns showed that the lattice parameter is 8.20 Å and structure is cubic spinel. Nickel- Zinc ferrite ($Ni_{0.5}Zn_{0.5}Fe_2O_4$) prepared by the Liu (2007). The particle size obtained by Liu was 9.5 to 94 nm, showing a dependence of the grain size with the calcinating temperature. Moumen in 1995 produced the nanoparticles with diameter of 5nm [21]. In 2008 Dong- Lin produces the Nickel- Zinc ferrite ($Ni_{0.5}Zn_{0.5}Fe_2O_4$) particles with the size between 0.4 to 4µm. The electrical, dielectric properties of the Nickel- Zinc ferrite are of great concern. There are so many applications pertaining to electrical and dielectric properties of the ferrites. A lot of research has been done on these properties. Dielectric constant, dielectric loss, ac and dc electrical resistivity are very based upon the crystal structure, grain size of the Nickel- Zinc ferrite. The crystal structure and grain size is depending on the process by which the material is formed.

AC conductivity ($\boldsymbol{\sigma}_{ac}$) increases by increasing the frequency. The dielectric loss is due to the imperfection and impurities in the crystal lattice. Dielectric constant (ε′) also increases on increasing the frequency. Up to 10 kHz the dielectric constant increases. On further increase in frequency the dielectric constant decreases. The reason for the change in dielectric constant with the frequency is that the ferrites conversion from ferromagnetic to paramagnetic on changing the frequencies. The dielectric constant (ε′) also changes with changing the temperature.

1.6 Advantage of Ferrites over other Magnetic Materials:

Magnetic materials like iron and metallic alloys have low values DC electrical resistivity making them unsuitable for high frequency applications. The matter arises from the fact that their high electrical conduction allows the currents that are induced to travel in the the material itself, generating heat and making the process inviable due to the energy losses which may cause serious environmental concerns. This loss of energy makes such materials inefficient especially at higher frequencies. Ferrites, on the other hand, have very high DC electrical resistivity and high permeability so they can perform better as wide band transformers, quality filter circuits, adjustable inductors delay lines. The use of ferrites is becoming more common specifically because of its performance at higher frequencies [1]. Ferrites are known to be cheaper than magnetic metals and alloys and may be considered the best core material choice for frequencies ranging from 10kHz to a few hundred MHz when one is limited by cost while demanding high inductor quality, high stability and low volume. Moreover, the flexibility of ferrites in terms of magnetic and mechanical properties is second to none.

1.7 Application of Ferrites:

Ferrite Nano- particles useful for applications involving high frequencies due to their high resistivity[6]. Ferrite Nano-particles have potential candidates due to their following properties:

- ✓ High efficiency at microwave frequencies
- ✓ Stability at high temperature
- ✓ High frequency applications
- ✓ Wide selection of materials
- ✓ High Coercivity (selective ferrites)

Ferrite Nano- materials are chosen due to their high DC electrical resistivity i.e. >106 Ω-cm, high magnetic properties, chemically stability and low eddy current losses. They may be used as:

- ✓ Microwave devices

- ✓ Inductor Core Material
- ✓ Electromagnetic absorbers
- ✓ Drug delivery
- ✓ Ferro-fluids
- ✓ Data storage

1.8 Introduction to Carbon Nanotubes:

In 1985 a researcher named Richard Smalley along with Robert Curl (Rice University) made an astounding discovery. Using a pulse of high intensity laser light, they struck the laser on a sample of graphite, vaporizing the carbon in the process. The vaporized carbon was carried to the mass spectrometer using a stream of helium gas. The peaks obtained by the mass spectrometer related strongly with a particular peak which indicated a cluster of 60 carbon atoms. The ease of which C 60 clusters were formed spurred the group on to proper a new allotrope of carbon. This new form was spherical in shaped and formed a total of 32 faces, 12 pentagonal and 20 hexagonal. Researchers kept experimenting with this new allotrope and soon discovered that the C60 configuration may also exist in a long cylindrical tubular form. These tubular carbon structures are now better known as carbon nanotubes or CNTs.

Carbon nanotubes is one of the allotropic forms of carbon consisting of cylindrical molecules with the approximate length to diameter ratio of 132,000,000:1. CNTs are extremely valuable in various fields of nanoscience and technology including the electronics and optical industry due to enhanced thermal conduction, electrical and mechanical properties. CNTs basically have a long and hollow structure with graphene sheets, one atom thick, rolled at chiral angles. The properties of CNTs may be determined by the radius and chiral angle. CNTs have unique properties due to SP^2 bonds; stronger than sp^3 bonds. Schematic diagram of CNTs is shown below[7].

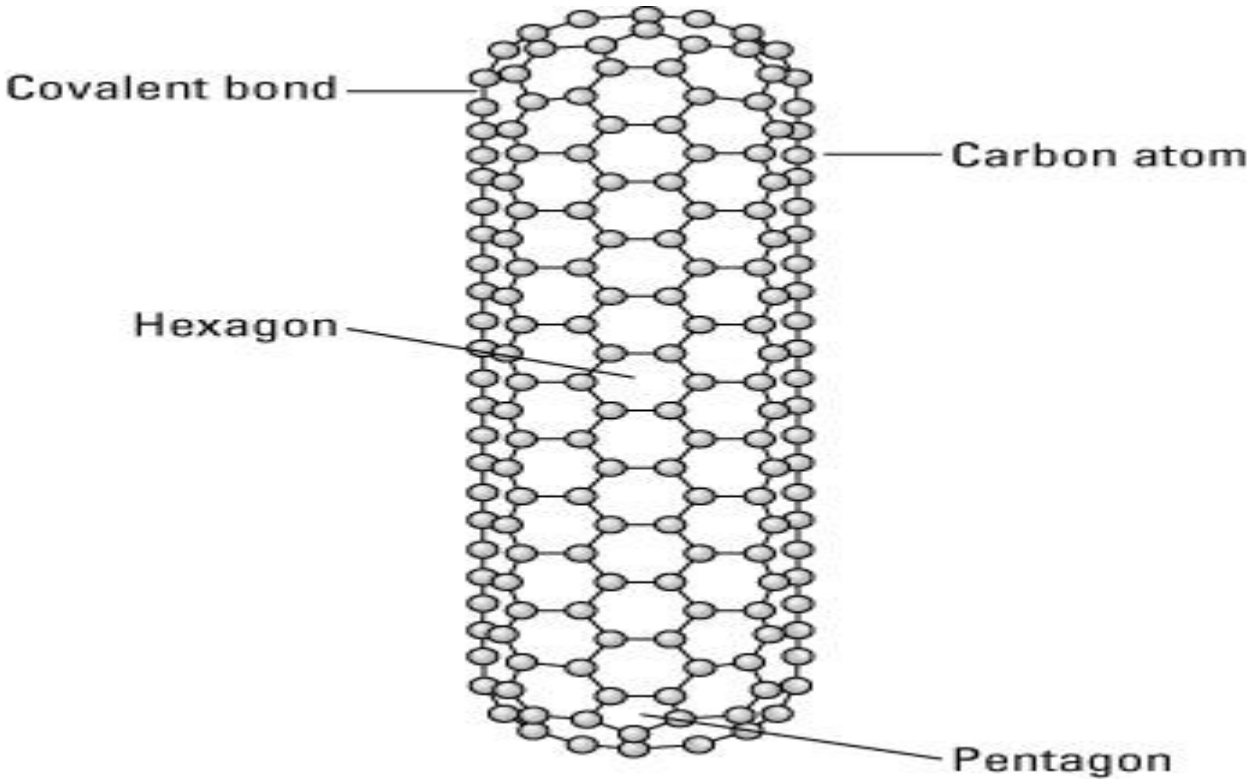

Fig1.7 (a): Basic Structure of CNT

(Adopted from: Wikipedia, "Introduction to Carbon Nanotubes")

1.8.1 Multiwall Carbon Nanotubes:

MWCNTs consists of multiple graphene layers rolled in the form of a scroll shape with diameters of the tubes ranging from 5nm to 50 nm. MWCNTs consists of several tubes within the same a cylinder with 6 to 25 number of walls. The distance of the interlayer walls is closer than that of the distance between graphene layers in graphite. MWCNTs have high aspect ratio with the length to diameter ratio being approximately 100:1.

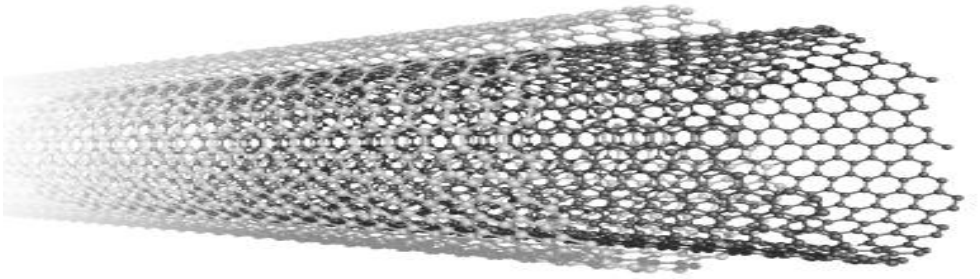

Fig 1.7 (b). Inside Lateral View of MWCNT

(Adopted from: Wikipedia, "Introduction to Carbon Nanotubes")

The properties of MWCNTs depend upon the degree of straightness and entanglement which in turn are functions of the dimension and the degree of defects in the tubes. The SP^2 bonds cause MWCNTs to be thermally stable up to 600 ^{o} C with high chemical stability. SEM image of MWCNTs is shown below[8].

MWCNTs have excellent properties which are being employed on a large scale in various industries along with commercial applications.

The properties of MWCNTs are:

- Electrical: MWCNTs are conductive by nature, but to make them efficient they have to be linked together in the composite system. One may take advantage of the fact the only the outer walls are responsible for conducting and not the inner walls.
- Morphology: MWCNTs have high aspect ratio, which means that their lengths are 100 times more than the diameter. Even though their properties are dependent upon this high aspect ratio, the characteristics are also based upon the

degree of entanglement of the tubes, which is the direct result of the defects in the tubes.

- Physical: MWCNTs have excellent tensile strength and integrating the tubes into plastics can further increase the strength.
- Thermal: MWCNTs have are thermally stable for just over depending upon the defects and impurities present in the tubes. Furthermore, the residual catalysts in the product helps decomposition of the CNTs above the said temperature.
- Chemical: MWCNTs have sp2 hybridized carbon, this is also found in graphite and like graphite it has high chemical stability as stated above by the high thermal stability. Furthermore, the CNTs can be functionalized to attach different molecules further enhancing the properties of the material.

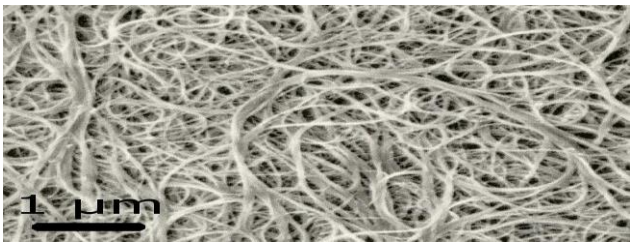

Fig 1.8 SEM image of MWCNTs

(Adopted from: Wikipedia , "An introduction to CNTs")

Application of MWCNTs include:

- Battery Cathodes
- Filtration Membranes
- Conductive Polymers
- Enhanced Carbon Fibers
- Spray Coated Heater Elements
- Heat Conduction Materials
- Optical and Electronic Industry

1.9 Nano- hybrid of $Ni_{0.5}Zn_{0.5}Fe_2O_4$/MWCNTs:

SP^2- hybridized elemental carbon may form a tube-shaped structure having a honeycomb atomic array, containing many shells of graphitic known as MWCNTs. Due to their unique structure, MWCNTs have remarkable thermal, dielectric and electrical properties and are widely applicable applications in material science. To fully use their capabilities, MWCNTs are embedded with different types of nanoparticles and synthesized using different techniques. Ferrite Nano- composites with MWCNTs are a suitable hybrid for dielectric and microwave absorption applications because of characteristics such as electromagnetic interference shielding, high permeability, high permittivity and dielectric losses. Ferrite/MWCNTs Nano-hybrid exhibiting ferromagnetic behavior at room temperatures have been reported by researchers [9]. Microwave absorption characteristics of ferrite nano composite with MWCNTs have gained much attention due to use in defense organization. Among the metal iron oxide nanoparticles, with the chemical composition of MFe_2O_4 where M is divalent metal ions, Nickel- Zinc ferrite has spinal hard magnetic material exhibiting significant optical, electrical and magnetic properties. Nickel- Zinc ferrite also has high chemical stability, corrosion resistance and economically friendly. Different synthesis routes for examples, Hydrothermal, Micro-emulsion, Sol-Gel, Solvo-thermal, Co-precipitation and etc. decorating of MWCNTs along with Nickel- Zinc ferrite, a wide range of properties may be achieved with potential applications in bio- medics and electromagnetic devices, drug delivery, magnetic data storage etc.

With the increasing environmental hazards owing to the burning of fossil fuels, we need to shift our energy sources from the burning of fossil fuel to a better, more environmental friendly source. Although electricity is a versatile form of energy, it has a huge disadvantage, that being, it is relatively difficult to store e.g. batteries can store large amount of electric power but they need a large investment of time to gain a complete charge. On the other hand, if we look at capacitors, they acquire a complete charge instantly but they can store only a relatively small amount of charge. In our near future, we need to devise a unit which can store and release huge amounts of electricity simultaneously. One way to do that is to enhance the dielectric properties of a material.

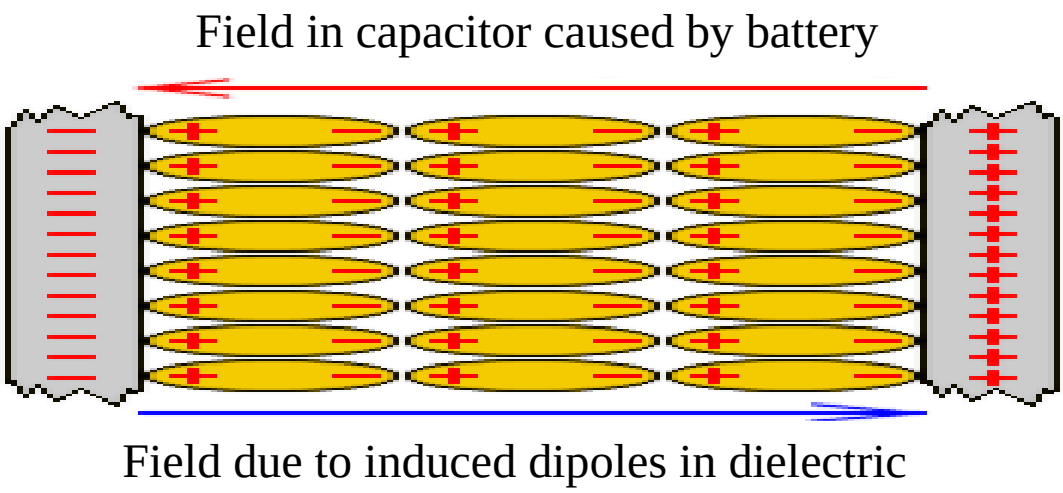

Fig 1.9: Dielectric Dipole Orientation

(Adopted from: Wikipedia, "Working of Capacitors")

Take into consideration two conductive metal plates which are electrically neutral and are separated by a distance 'd'. Connecting these plates to a battery of a certain potential, the anode terminal of the battery will negatively charge the plate in contact with it while the cathode will positively charge the plate in contact with it, thereby creating a potential between these plates. Since, there is no direct or conducting contact between the plates, no charge will flow, thereby creating a potential between the plates. If we remove the battery, the plates will remain charged with the ability to do electric work. Here, the non-conducting or insulating material between these plates, maintaining said distance 'd' is called a dielectric material. The dielectric material performs two functions; allowing the charges to keep at bay from each other, thus creating a potential while also allowing the electric field generated by the potential between the plates to do additional electric work to align its dipoles along the lines of force of the field, thus giving the capacitor the ability to store more electric work or charge as shown in the Fig1.9, owing to its high dielectric value. Increasing the surface area of plates, hence increasing the dipole moments per unit area, this ability of the dielectric material maybe enhanced. In our present study of Nano- hybrid, MWCNTs offer high surface are acting as conductive plates, thus storing more charge on them while the Nickel- Zinc ferrite nanoparticles will act as a dielectric medium in between the MWCNTs.

Chemical Co-precipitation was employed for manufacturing of Nickel Zinc Nano-ferrite particles. Uniform dispersion of the MWCNT's was achieved using Ortho-xylene and complete homogenization of Nickel- Zinc ferrite nanoparticles was ensured by following a solid state method. The formation single phase along with the presence of MWCNTs was confirmed by XRD and SEM. The electrical Properties were studied using Agilent E4991A material analyzer. This study would present a relatively simple method for the synthesis of ferrite/MWCNTs Nano-hybrid with improved electrical properties as well as microwave absorption characteristics which can be deployed in electronic industry.

1.10 Objectives:

The present work is carried out with following objectives

- Synthesis of single phase spinel ferrite nanoparticles of $Ni_{0.5}Zn_{0.5}Fe_2O_4$ using an inexpensive and simple chemical Co-precipitation
- To synthesize $Ni_{0.5}Zn_{0.5}Fe_2O_4$ / MWCNTs composite using xylene as a dispersive medium
- To study different loadings of MWCNTs in $Ni_{0.5}Zn_{0.5}$Fe2O4 ferrite nanoparticles and their effect on the dielectric properties.

Chapter: 2

Theoretical Review

2. Approaches to Nanoparticle Synthesis:

The patterning and preparatory methods of nanostructured species are founded in well-designed techniques. These techniques and their preceding modifications can be broadly placed into “the top down” and “bottom up” approaches.

2.1 Bottom-Up Methodology:

In the Bottom-up methology, the short-range fundamental forces guide the process of assembly of atoms and molecules as starting factors, employing the principle of chemical recognition. Thus the chemical assembly of atoms or molecules using thorough understanding of short-range intra and intermolecular forces of attraction at play, like electrostatic forces, Van der Waals forces constitutes the bottom up approach. This approach allows for control of morphological control and a certain order of chemical ‘versatility’. Examples of this approach include colloidal dispersion, chemical vapor growth and self-assembly.

2.2 Top-Down Methodology:

The top down methodology flips the bottom up approach by employing large entities in bulk and break them down into smaller ones, forgoing atomic-level control. Using microfabrication methods and moving towards a nanometer size-regime, a stark abrupt change in the characteristics like optical, physical, electrical, thermal and mechanical properties is observed. The materials exhibit different properties at nano-regime, compared to their macro-counterparts. These changes are attributed to increase in surface to volume ratio, lowering of grain size, increment in grain boundary junctions, pores and interfaces. Also, defects are generated in constituting atoms and lattices through this approach. Some opaque materials become transparent at nanoscale (for example: copper). Gold is insoluble at macro-size but becomes soluble at nano-scale.

Changes in reactivity and ion transfer are observed as well. The popular examples of this technique include surface modification, lithography, vapor treatment and etching and patterning techniques like photolithography and ink-jet printing.

2.3 Synthesis Techniques of Nanoparticles:

Synthesis of nanoparticles through different methods, allows for tweaking of electric, magnetic and morphological functionalities. Some of the widely used methods are stated below:

- Chemical Co-Precipitation Method
- Hydrothermal Method
- Micro-Emulsion Method
- Gas Condensation Process
- Sol-gel Technique
- Combustion Flame Synthesis
- Sono Chemical Method
- Poly Vinyl Alcohol (PVA) Evaporation Method
- Solvothermal Synthesis

Sol-Gel Method allows for complete homogeneity and is cost effective. Using this method, the product formation at low temperatures can be controlled. The particles obtained through this method find applications in optics and electronics. Poly Vinyl Alcohol (PVA) evaporation method is cost effective as PVA is cheap and readily available. This method produces uniformly sized particles. Gas condensation process utilizes inert gas at high pressure in a vacuum chamber. This method is not suitable for the production of spherical particles.

Large scale production of nanomaterials is achieved through flame processes. It has the advantage of being a one-step process with no machinery required to be mobile. The important drawback of this method includes the lack of control over the nanoparticle functionalities [10]. The micro-emulsion technique**,** reverse micelle is formed through dissolution of surfactant in organic solvent. The surfactant molecules are surrounded by water molecules, effectively forming a micro-scale reactor for nanoparticle synthesis.

Precipitation step allows for production of fine ferrite nanoparticles in these micro-sized water-in-oil reactors [11]. The sono chemical method is carried out under ultrasonic waves, where starting materials react with each other. The major advantage of this method is the size reduction and low size distribution. The morphological properties can be controlled and uniformity of dissolution is achieved [12]. The hydrothermal/solvothermal methods are simple and effective processes that allow for a remarkable control over particle morphology by control over recrystallization. Various nanocrystals, nanorods, hollow spheres, urchin-like crystals can be synthesized through this cost effective and easy method.

The current research employed co-precipitation methods for the formation of copper ferrites, hence the process is explained in detail below.

2.4 Introduction to Chemical Co-Precipitation Method:

The chemical co-precipitation method has become the choice method for production of nanoferrites as it allows for synthesis in a short duration. The known disadvantages of this method include the emission of fumes as well as the lack of control over the particle size beyond a known range. Simply put, the reactants are dissolved in water in the ratios determined by the protocol. The solution pH is maintained by addition of sodium hydroxide. The initial precipitation process leads to nucleation of particles but it is rapidly replaced by thermodynamically stable and desirable growth. In order for the co-precipitation to occur in the medium, the nucleation rate should exceed the growth rate [13-18].

The method is significant, chiefly because it is cost effective and easy and the resultant product is fairly homogenous and pure. The crystallinity of the nanoparticles is influenced by impurities and rate of reaction of the employed synthesizing method. The nanoparticle shape, size and morphology is affected by super saturation affects, growth rate and nucleation. Particle size reduction is observed in cases where super saturation is high. The reaction parameters such as rate of reaction and transport of chemicals is dependent upon concentration of starting reactants. The degree of precipitation is dependent on factors like temperature and pH.

2.5 Chemical Co-Precipitation Method Explained:

This method is often adopted to synthesize Nano powders of electro ceramics, forming complex oxides, disadvantages accompanied with this technique are emission of fumes. Co-precipitation reaction revolves around the simultaneous occurrence of nucleation, growth, coarsening and/or agglomeration process. Nucleation starts when the many molecules present in the reaction solution combine together and start forming the initial crystals, as the reaction proceeds the other molecules join together with the nucleus becoming chemically stable and in turn, providing thermodynamic stability to the nucleus. Many such nuclei are formed all throughout the reaction solution and are grown simultaneously. The remaining molecules present in the reaction solution are attracted to more thermodynamically stable larger particles and hence, the particles grow, the stated process is known as coarsening. In order to obtain nano sized particles the nucleation of the particles must be relatively fast while the growth of the said particles is supposed to remain relatively slow, this would ensure that the nano sized nucleus would not grow out of the nanoparticle range. If one is to achieve a uniform size distribution of the particles, then the process must be controlled as such that all the nuclei are formed simultaneously, that is at the same time, so that their growth and further coarsening may not hinder the size distribution. Going further into the process, there are three main mechanisms of co-precipitation: inclusion, occlusion and adsorption. An impurity, having the ionic radius and charge similar to that of the original atom, occupying a lattice site in the crystal, kicking out the intended atom is known as an inclusion. Adsorption is a surface reaction in which the impurity, regardless of the radius or the charge is bounded to the surface of the precipitate. The bond that exist is usually weak Van der Waals. And ad- sorbate may lead to the third type of co-precipitation which is occlusion. This occurs when the ad-sorbate particle gets physically trapped inside the crystal, this may happen due to the growth of the crystal around the adsorbed impurity. Reaction for synthesis of oxides are separated in two categories. The first process produces the oxides directly; no further treatments are required to cleanse the particles apart from the washing out of the ‘toxic’ resulting products which may hinder in the gathering of ultra-pure powders. The second process produces a metal hydroxide precursor that has to be further processed and purified in order to obtain the final oxide sample. The washing process is imperative in

both the aforementioned cases as the resulting salt has to be washed away. In the latter the hydroxide is calcinated (heat treated) so that the hydrogen may drift away leaving the pure metal oxid.. Co-precipitation method is a wonderful method to create fine particles of nano size[19-24]**.** It is quite efficient to obtain ferrites with the help of co-precipitation method because the ferrites are pure and homogeneous in their chemistry. Under fine control of pH using NaOH; various salts like sulphates, nitrates and chlorides result into the oxide nanoparticles in a co-precipitation process. In co-precipitation process the particle size is dependent upon the pH of the starting precursors and the molarity of the chemicals.

Concentration of the chemicals affects the transport and chemical rates. The reaction rate and the impurities affect the crystallinity of the particles. Particle shape size is affected by factors including growth rate, nucleation and super saturation. At high super saturation the particle size is small and at high super saturation the size of particle becomes small. Mostly NaOH is used as precipitating agent [25-29]. A reasonable value of pH and temperature is required for the precipitation purpose. The whole process for the co-precipitation can be shown in Fig 2.1.

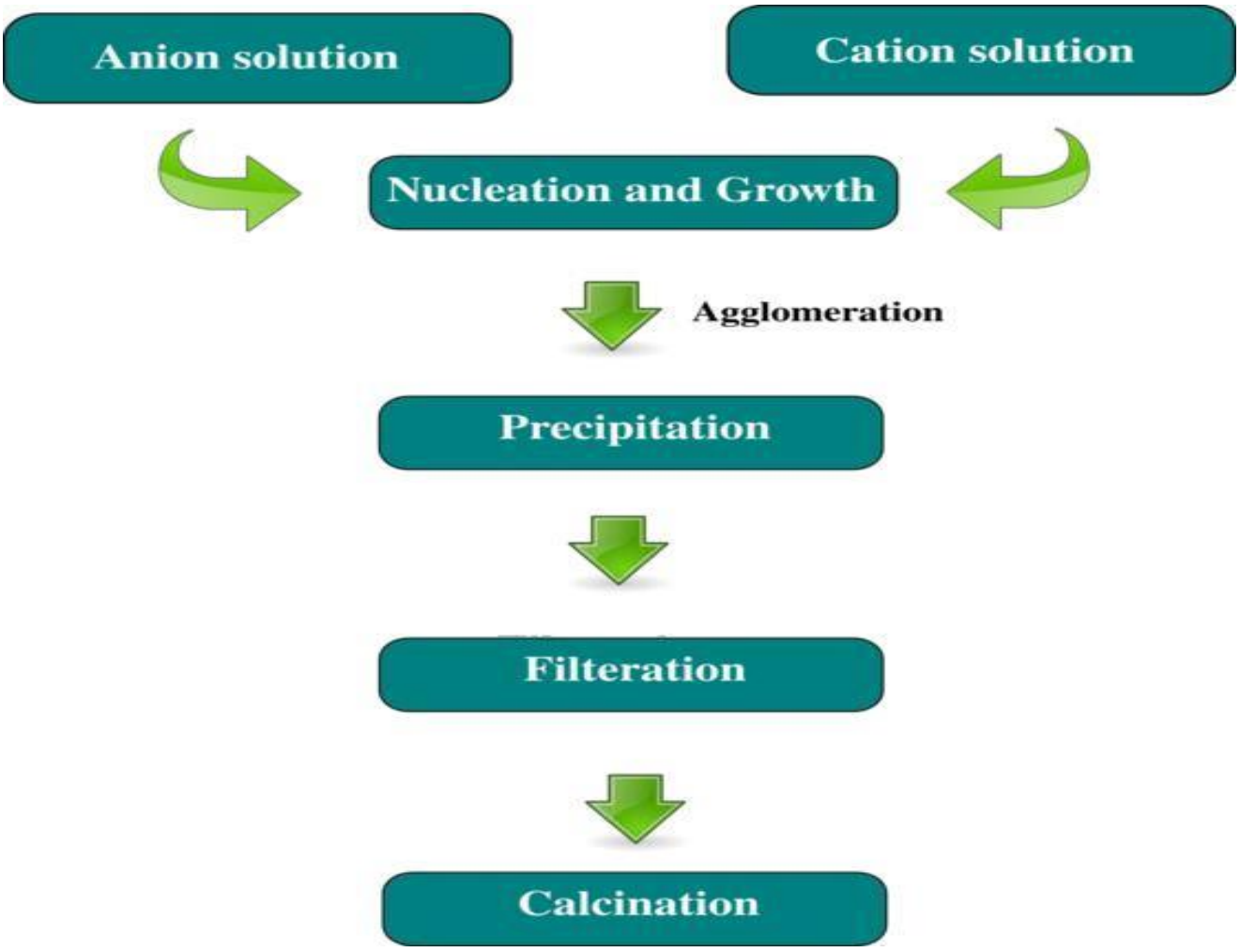

Fig 2.1 Chemical Co-precipitation steps

(Adopted from : Nucleation Processes in Catalysis , Volume 2)

2.5.1 Major steps in Co- Precipitation:

Two major steps involved in co-precipitation are:

- Co-precipitation step
- Ferritisation step

2.5.1.1 Co- Precipitation step:

Metal hydroxides in the form of colloidal particles are attained by the co-precipitation of metal cations in alkaline medium. For the case of Ni-Zn ferrites this reaction is:

$$(Ni(NO_3)_2.\ 6H_2O) + Zn(NO_3)_2\ .\ 6H_2O + Fe(NO_3)_3.\ 9H_2O + NaOH$$

$$\Downarrow$$

$$Ni(OH)_2.\ Zn(OH)_2.\ Fe(OH)_3 + NaNO_3$$

2.5.1.2 Ferritisation Step:

The product is heated in the precipitation alkaline solution to transform the metal hydroxides solution to the Ni-Zn ferrites

$$Ni(OH)_2.\ Zn(OH)_2.\ Fe(OH)_3 + NaNO_3$$

$$\Downarrow$$

$$Ni_{0.5}Zn_{0.5}\,Fe_2O_4.\ nH_2O + (4\text{-}n)\ H_2O + NaNO_3$$

The ionic impurities of Na and NO_3 are removed by washing the product with deionized water until the pH value reaches to neutral.

2.6 Parameters involved in Co- Precipitation:

Parameters with influence on the co-precipitation process are described below:

1. Rate of mixing of the reactants
2. Role of anion
3. Temperature effect
4. Effect of pH
5. Heating after co-precipitation

2.6.1 Rate of mixing of the reactants:

The rate of mixing greatly influenced the size of the particles. If the growth rate is slow and the nucleation rate is higher than the growth rate, then small size of the particles is achieved and vice versa. In first case the rate of mixing of the precursors is very high and in the second case rate of mixing is low[30-34]. Slow mixing gives the particles of homogeneous chemistry.

2.6.2 Role of Anion:

Anions may be in the form of metal ion solutions of in the form of salts. For good results the use of the metal salts is recommended. The metal salts used in Co- precipitation are sulphates, nitrates or chlorides. These salts are chosen on the basis of being able to be easily separated from the final product, usually by washing or decomposing during the heat treatment process. As a general thumb rule, nitrates and carbonates salts are used as metal precursors due to their ability to easily leave the metal ion. Combined with ammonia or sodium carbonate as the precipitating agent. Chloride and Sulphates act as poison ions which should be avoided as they hinder in the production of high purity particles.

2.6.3 Temperature Effect:

Different values of activation energy are required for different metals to achieve ferrite formation. The heat energy provided to the reactants acts as the activation energy. For the formation of nickel- zinc ferrites, the reaction temperature is kept in the range of 70-100 ^{o}C. This temperature range is imperative in controlling the crystallite size and hence

the surface area of the particles formed. Researchers have found it very hard to pin point the exact effect of the temperature of precipitation with results varying greatly, however, it has always been found that the nucleation rates are dependent upon the temperature. This may be traced to the specific kinetics of the process in question and the activation energies of the reagents in the reaction solution. Some cases point towards the temperature controlling the nucleation process while other studies show and added rate of the growth and coarsening mechanism.

2.6.4 Effect of pH:

PH plays a significant role in the synthesis of controlled size and shape particles. The pH of a reaction system controls the degree of super saturation of the nanoparticles in the reaction solution, therefore, is said to have a major effect on the final properties of the nanoparticles formed. However, there is no general rule of thumb, and the effect of pH for every reaction is different and has to be studied for every system. As an example, in the Zinc oxide thin film deposition system, a film formed below the pH value of 8 is porous and almost opaque, while a film formed above the pH value of 13 is said to be milky white and almost without defects, however, studies showed that the best results were obtained at pH values between 11 and 13. This is due to the change of the phase being formed and even the effect that the pH has on the reaction kinematics. At low values of pH, the significant growth of particles is not achieved. Increasing the value of the pH; the growth rate of the particle is high enough. Increase in the pH value decreases the time required for the synthesis of the product. In our case of Nickel- Zinc ferrites, the pH range is 8-10.

2.6.5 Heating after Co- Precipitation:

Annealing is required for achieve the desired phase of the final product. The temperature and duration of heating is important as it controls the size and shape of the particles. Chemical co-precipitation process has many advantages over other synthesis techniques.

- Mono-dispersed and homogeneous particles formation

- Rapid and simple preparation of particles
- Particle shape and size are easily controllable
- Particle composition is also controllable

2.7 Synthesis of $Ni_{0.5}Zn_{0.5}Fe_20_4$:

For the preparation of nominal composition $Ni_{0.5}Zn_{0.5c}Fe_20_4$, the chemical reagents used for Co- precipitation were iron nitrate along with NaOH to control the pH in range 8-10 for the co- precipitation to occur, which is then subsequently neutralized by washing the sample with de-ionized water. The respective composition was made using the simple stoichiometric formula:

$$\text{Mass} = \frac{\text{Molarity X Molecular Mass X 100}}{1000}$$

The chemical co-precipitation method has become the choice method for production of nanoferrites as it allows for synthesis of powdered ferrites in a short duration. The known disadvantages of this method include the emission of fumes as well as the lack of control over the particle size beyond a known range. Simply put, the reactants are dissolved in water in the ratios determined by the protocol. The solution pH is maintained by addition of sodium hydroxide. The initial precipitation process leads to nucleation of particles but it is rapidly replaced by thermodynamically stable and desirable growth. In order for the co-precipitation to occur in the medium, the nucleation rate should exceed the growth rate.

The method is significant chiefly because it is cost effective and easy and the resultant product is fairly homogenous and pure. The crystallinity of the nanoparticles is influenced by impurities and rate of reaction of the employed synthesizing method. The nanoparticle shape, size and morphology is affected by super saturation affects, growth rate and nucleation. Particle size reduction is observed in cases where super saturation is

high. The reaction parameters such as rate of reaction and transport of chemicals is dependent upon concentration of starting reactants. The degree of precipitation is dependent on factors like temperature and pH. The product was allowed to go back to room temperature and cleansed with double distilled deionized water for many cycles to get Nickel- Zinc ferrite particles with no impurities as a precipitate associated with a small amount of water content that was eliminated; dry powder of Nickel- Zinc ferrite nanoparticles was acquired by overnight dehydrating at 100 ^{o}C in the oven. The powder was further calcinated at 800 ^{o}C using Muffle Furnace for six hours to remove the carbonaceous impurities to obtain a well distinct spinal phase. The resultant powder was grinded using a Mortar and Pestle to eliminate agglomeration and the powder was characterized using X-rays Powder Diffraction, Two Probe Method and Scanning Electron Microscopy. In terms of calculating dielectric properties, the powder was forced by the hydraulic press. The applied pressure was three tons and the round cylindrical pellet was obtained.

2.8 Xylene as a Dispersive Medium:

Xylene is an aromatic hydrocarbon consisting of a benzene ring with two methyl groups attached at different position, with the molecular formula of C_8H_{10}. It has three isomers as shown below:

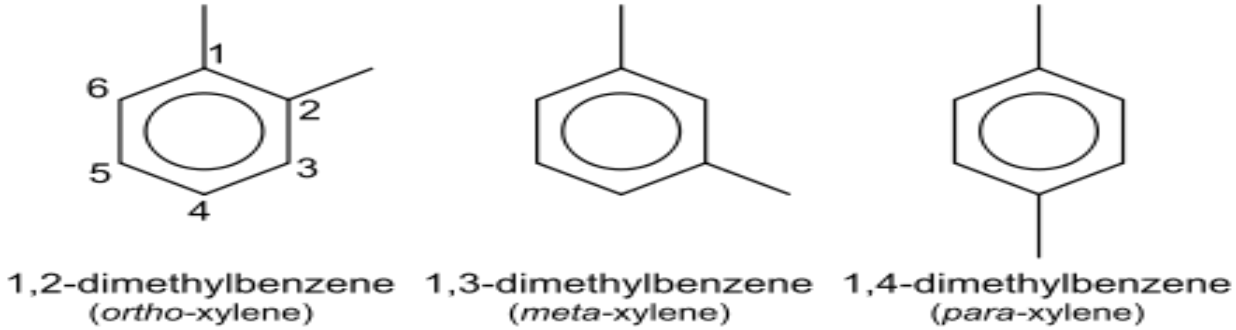

Fig 2.2 Isomers of Xylene

Adopted from: Wikipedia, "Xylene as a solvent"

The name 'Xylene' was initially coined by Auguste Cahours, in 1850 having been seperated as a constituent from wood tar. Xylene is a colorless and greasy liquid often used as a solvent/dispersive medium due to the following reasons:

- ✓ Density of each isomer is 0.87g/mL, lower than water, rendering xylene a suitable candidate for dispersion.
- ✓ Xylene has a benzene ring structure, which entails the sharing of the electron between the six carbon atoms in the ring, other electrons within the molecule's bonds get attracted towards the ring structure. As Nickel- Zinc also has the tendency to give up electron, achieving valence state of ($Ni_{0.5}Zn_{0.5}^{+2}$, $Ni_{0.5}Zn_{0.5}^{+3}$) and for iron to achieve valence state of (Fe^{+2}, Fe^{+3}), a weak polarization or Van der Wall forces develop, resulting in complete mixing and dispersion of MWCNTs and Ferrite particles.

2.9 Synthesis of Nickel Zinc ferrite/MWCNTs Nano- hybrid:

To prepare ferrite nanoparticles/MWCNTs Nano- hybrid, MWCNTs and Ni-Zn ferrite nanoparticles were mixed separately with 100 ml of ortho-xylene and many hours at room temperature were sonicated. The ferrite particles were augmented to MWCNTs dispersion and the resulting mixture was again sonicated for 12 hours using ultra-sonication. The weight percentage of MWCNTs was altered (0%-5%) in order to evaluate the increased loading consequence of MWCNTs on magnetic, electrical and dielectric properties of the prepared composite.

The overall procedure for the experimentation in a flow chart shown on the next page.

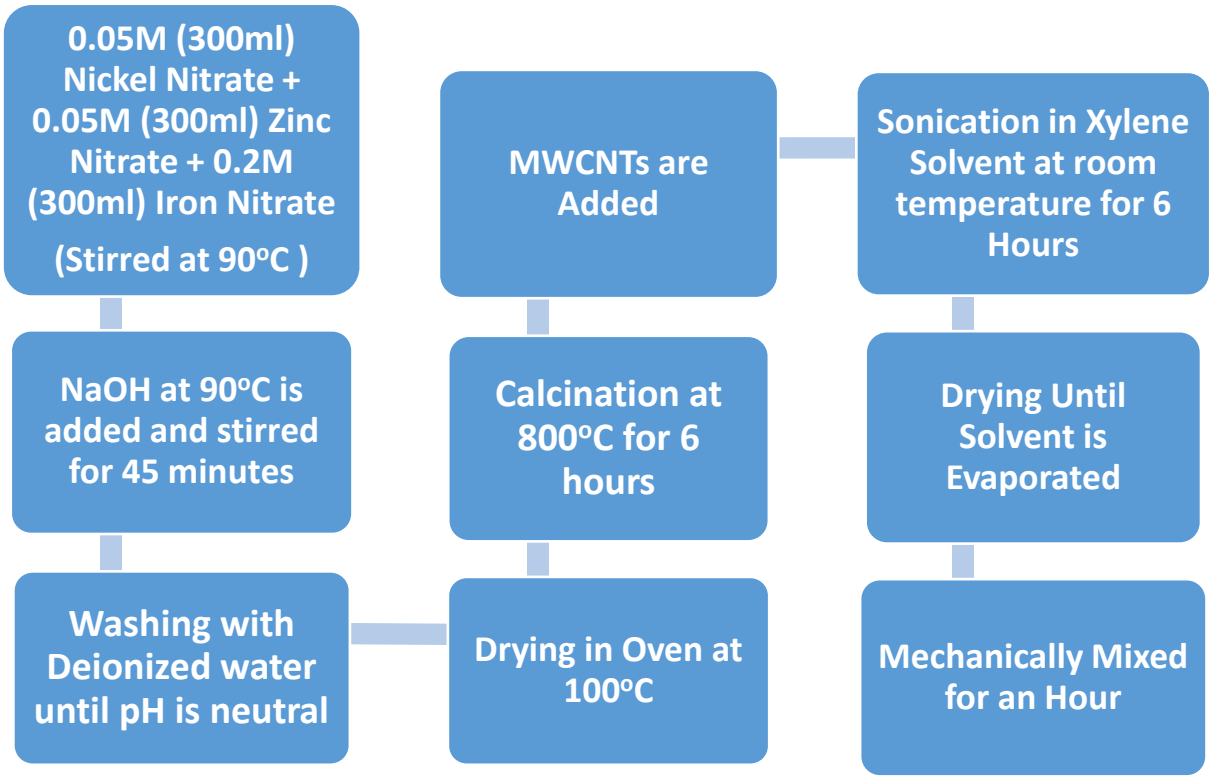

Fig 2.3: Experimental Work

Chapter: 3

Introduction to Sample Characterization Techniques

3. Characterization Techniques

In order to analyze varying properties of the Ferrite nanoparticles coated MWCNTs, some specific scientific methods are essential. Each method is unique in its ability to provide specific data regarding structural geometry, physical and chemical properties. A brief introduction to these methods is explained in this chapter. The materials synthesized are characterized by different methods as follows:

A) Morphological studies:

(i) X-Ray Diffraction Technique

- ❖ Porosity analysis
- ❖ Lattice parameter calculation and particle size
- ❖ Phase confirmation
- ❖ X-ray calculation and mass density determination

(ii) Scanning Electron Microscope

- ❖ Properties of surface morphology
- ❖ Elemental analysis

B) Electrical Characterization:

(i) Impedance Analyzer

- ❖ Dielectric properties
- ❖ DC resistivity measurement at room temperature
- ❖ AC conductivity
- ❖ AC impedance spectroscopy

3.1 X-Ray Diffraction Technique

X-ray diffraction method was first designed by W.C. Rontgen in 1985. The crystal structure is incompatible with wavelength of light wave; hence it cannot be analyzed in light rays. The wavelength of x-rays on the other hand, are almost equal to slit-size within crystal and hence provide remarkable details of phase identification within crystal structure. X-ray diffraction method gives an accurate account of structural features, atomic spacing and unit-cell dimensions in a crystal.

The technique utilizes the wave-particle duality of x-rays and employs this duality to analyze degree of crystallinity and morphology of crystal structure through diffraction patterns. This method gives its users a precise understanding of defects in crystal, average crystallite size, crystallographic orientation, phases, structural strains and degree of crystallinity. The sample is finely ground before use. Different target materials can be employed, like Cu of Kα = 1.54 (used in current study) and molybdenum. The preparation methods can be classified into powder diffraction method, rotating crystal method as well as Laue method. The powder diffraction method is utilized most commonly and encompasses the following steps:

1. Diffractometer method
2. Debye-Scherrer method (formula)

3.1.1 Working Principle of XRD

The sample is required to be finely ground into a powder form. As the X-rays interact with the finely grounded sample, the plane at which x-rays are incident, act as a mirror and reflects the incident rays. The angle of this reflection is found to be equal to the angle of reflection for each set of atoms. Consequently, a constructive interference is attained in the crystal structure which can be further understood by Bragg's law equation:

$$n\lambda=2d\sin\theta$$

Where, n is the interference order, λ denotes wavelength of incoming x-rays, d specifies interlayer distance, θ represents the angle of incoming x-rays.

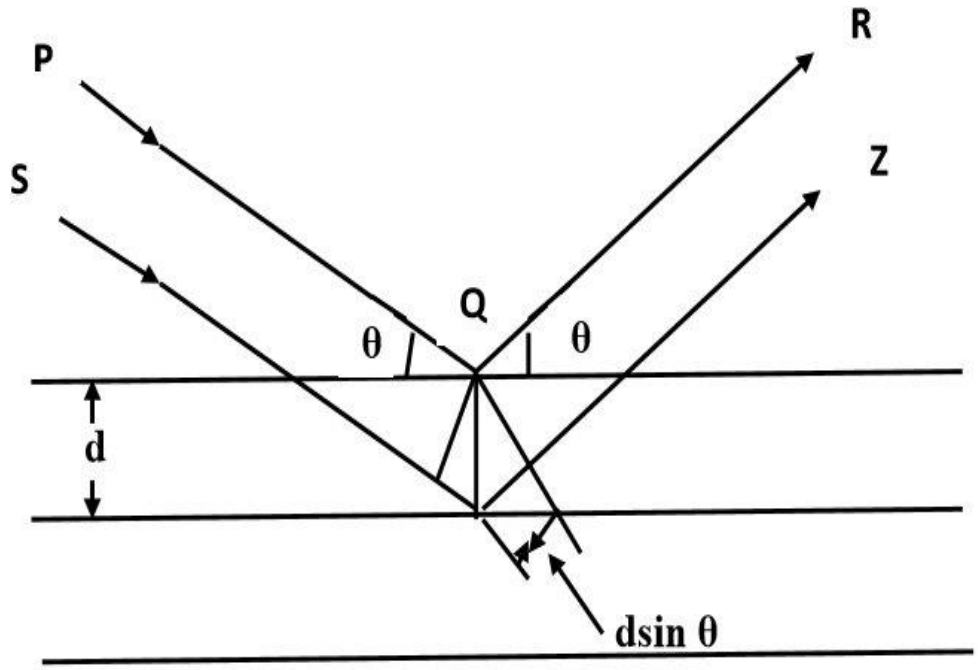

Fig 3.1: Scattering of Incident Beams of X-rays in crystal [35]

The equation specifies that, when incident rays are incumbent on the equally spaced/distanced crystal planes and are reflected, the difference between these planes have path difference equal to 2dSinθ. The value of θ is measured from the plane. Utilizing Bragg's law equation 2dsin θ =nλ, the diffraction is achieved only when the wavelength of incident rays is smaller than 2d. Hence λ<2d. This explains why photons from the visible light cannot be employed for this technique. Three dimensional analysis of structures can be done by using three sub-techniques namely:

(i) Powder diffraction method
(ii) Laue Method
(iii) Rotating Crystal Method

The current study only employs the powder diffraction method, as the sample is finely ground to a powder with particles in the nano scale and the pre-requisite single crystals of optimum size are unavailable. The grounded sample is placed in a circular or rectangular shaped glass plate or aluminum plate. As the x-rays are incident on the

sample, the nanosized particles act as randomly oriented crystal. Observing a singular reflection plane, it can be observed that the nanoparticle alignment in hkl plane completely fulfils the Bragg's angle. The diffraction cone of radiation formed when θ is kept constant. Knowing the exact values of 'θ' and 'λ' allows for accurate calculation of inter- planer spacing 'd'.

3.1.2 Lattice Constant

Lattice parameter, also known as lattice constant is denoted as a physical dimension of unit cell residing within crystal lattice. Within the 3d (three dimensional) lattices, three lattice constants are known to exist, denoted as 'a', 'b' and 'c'. The angle between the edges or length of a single edge within the crystal is given by the value of lattice constant. It is represented by the formula:

$$a= \lambda (h^2+k^2+l^2)^{1/2} / 2\mathrm{Sin}\theta$$

Where a= lattice constant, λ = wavelength of X-ray radiation (1.54 for Cu kα), h, k, l = miller indices and θ = diffraction angle.

3.1.3 Crystallite Size:

The crystallite size is parameter that receives great focus as it determines and predicts other parameters through its magnitude. The phase confirmation and phase identification is done by comparing the obtained diffractograms with JCPDS or pdf cards. Presence of broad peaks in a diffractogram pertains to the small crystallite size and vice versa. The Debye Scherer equation proves the peak width and crystallite to be in an inverse relation to each other, as is depicted by the following relation:

$$t = \frac{0.9\lambda}{\beta \cos\theta}$$

Here, t= crystallite size, λ =wavelength of the used X-rays, θ= diffraction angle, β= FWHM value of respective peaks.

3.1.4 X-Ray Density:

The values of x-ray density are dependent on lattice characteristics. When the value of lattice constant is known, the x-ray density can be calculated by the following formula:

$$\rho_x = ZM / N_A a^3$$

Here ρ_x = X-Ray density, M = molecular weight of sample, N_A = Avogadro's number (6.022×10^{-23}), a = lattice constant, Z = formula unit of cell.

X ray density studies depict that each unit cell in a spinel ferrite lattice is further divided into 8 formula units. X-ray density exists in an inverse relation with the lattice constant and a direct relationship with the molecular weight.

3.1.5 Bulk Density:

The measured density of the material is denoted by bulk density which relies on internal structure of the sample material. The sample is modified into circular pellets through a hydraulic press, in order to calculate bulk density. The value of bulk density is calculated by traditional formula for density given as:

$$\rho_m = m/\pi r^2 h$$

Here, where ρ_m = bulk density, m = mass, r = denotes radius, h = thickness of the pressed pellet sample.

3.1.6 Porosity Fraction:

The parameter of fraction of porosity is determined through the known values of bulk density and x-ray density. It is given by the formula stated below.

$$\rho_m / \rho_x$$

Here, ρ_m = bulk density, ρ_x = X-Ray density of the sample

3.2 Introduction to Scanning Electron Microscopy:

It is one of the many electron imaging techniques which provides imaging of sample surface as well as the bulk using a high energy beam of electrons. This high energy beam after interaction with the sample provides us valuable information like:

- Sample surface topography
- Composition of the sample
- Phase mapping

Many different types of signals are emitted by various interactions of beam with the sample surface including characteristic X-rays, back scattered electrons, secondary electron, transmitted electrons and cathodoluminesence, these signals are received by various detectors and fed to the computing system.

3.2.1 Principle of SEM:

In the scanning electron microscope, the beam of electrons is focused on the sample's surface in a very narrow cross sectional area. When electrons interact with the surface its interaction causes the emission of electrons or photons from the surface. These electrons and photons are gathered using different set of detectors and their output can be used to control the brightness of Cathode Ray Tube whose X and Y inputs are controlled in accordance with the X and Y voltages mastering the electron beam which ultimately results in generation of an image on the Cathode Ray Tube display; every point the beam impinges, is mapped on the CRT display. We get three types of images by SEM: Secondary electron images, backscattered electron images and elemental X-ray maps [17].

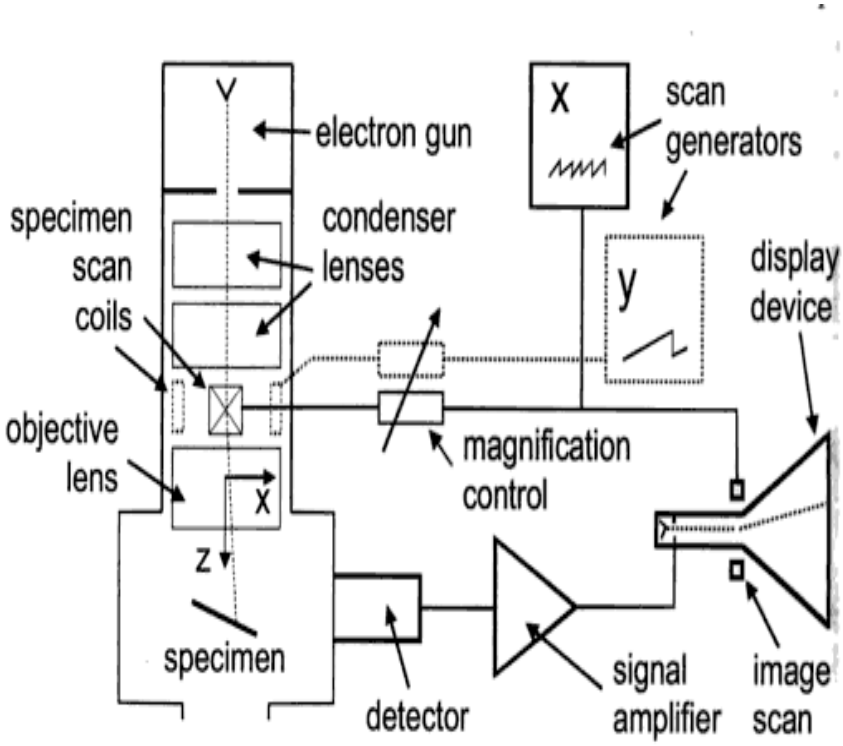

Fig 3.2 Schematic diagram of Scanning Electron Microscope with CRT display

(Adopted from: Materials Characterization: Introduction to Microscopic and Spectroscopic Methods, 2nd Edition Chapter 12: Working of SEM)

3.3 Electrical Properties:

3.3.1 Dielectric Properties

The dielectric characteristics i.e. dielectric constant and dielectric loss factor were determined using LCR meter bridge. **Capacitance** of the pellets was determined from the LCR meter and then **dielectric constant** was calculated using the formula

$$\varepsilon' = Cd/(A\,\varepsilon^0) \quad (3.9)$$

Where 'C' is the capacitance of the pellet, 't' is the thickness of the pellet in meters, 'A' is the cross-sectional area of the flat surface of the pellet and ε_0 is the constant of permittivity for free space and is equal to 8.85×10^{-12} F/m.

While the imaginary part corresponding to energy dissipation losses is calculated by using the equation:

$$\acute{\varepsilon}'' = \acute{\varepsilon} * D$$

In any dielectric material there exists power loss because of the work done to overpower the frictional damping forces faced by the dipole during their movement [26-28]. The **dielectric loss tangent (tan δ)** can be determined in terms of real (**$\acute{\varepsilon}'$**) and imaginary (**$\acute{\varepsilon}''$**) parts of dielectric constant as:

$$\tan\delta = D = \acute{\varepsilon}''/\acute{\varepsilon}' \quad \ldots\ldots\ldots\ldots (3.10)$$

While AC-Conductivity resulting because of the hopping mechanism is calculated using the equation:

$$\sigma_{AC} = \omega\varepsilon^0\varepsilon'\tan\delta \quad \ldots\ldots\ldots\ldots (3.11)$$

Chapter: 4

Results and Discussion

4.1 X-ray Diffraction (XRD) Results:

The Powder X-Ray Diffraction Technique was used to investigate the structure and phase formation of the prepared Ferrite/MWCNTs nano-hybrid.

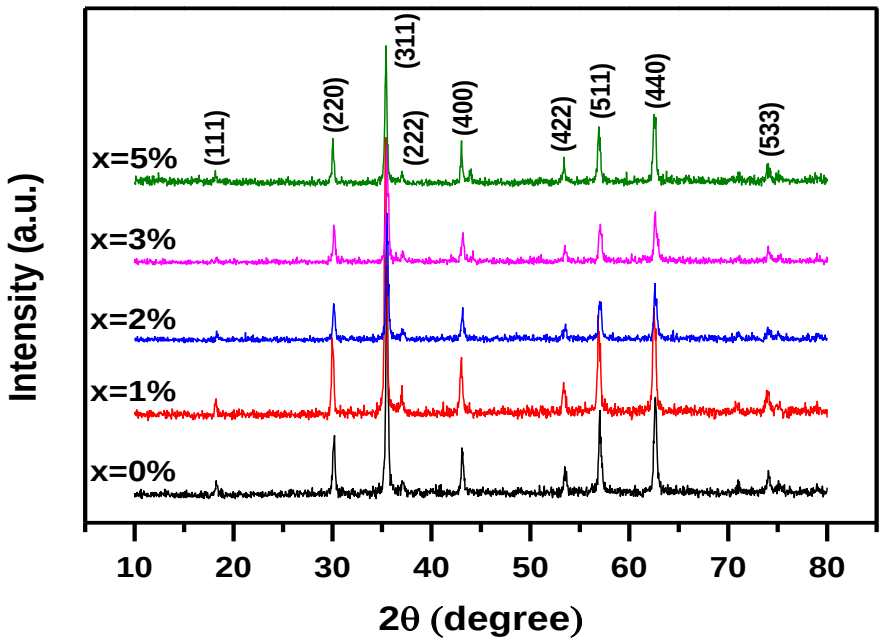

Fig4.1: XRD of Ferrite (0%, 1%, 2%, 3%, 5% MWCNTS)

The X-Ray powder Diffraction of the pure ferrite powder (fig 4.1), calcinated at 800^{o}C for 6 hours showed that the final product is $Ni_{0.5}Zn_{0.5}Fe_2O_4$ nanoparticles with the expected closed packed face centered cubic arrangement structure[19] in accordance with JCPDS card No.00–044-1485.The peaks referenced were (220), (311), (400), (511), (440). The appearance of the peak (3 1 1) at 35.760^{o} shows crystallinity of the synthesized product while the broadness FWHM (Full Width Half Maxima), in this case

the (311) peak, shows the formation of a small crystallite size which in turn confirms the formation of small grain size. The additional peaks observed maybe attributed to hematite phase constituting of unreacted Fe_2O_3. Using the Debye Scherer formula, the crystallite size was calculated to be between 22nm to 56nm.

The XRD patterns were obtained for the synthesized nano-hybrid. All the samples showed well resolved diffraction peaks located at $2\theta = 30.14^o, 35.51^o, 43.15^o, 57.09^o$ and 62.68^o corresponding to their respective planes (2 2 0), (3 1 1), (4 0 0), (5 1 1) and (4 4 0) which confirms the formation of face centered cubic spinel phase. Some important characteristics of the XRD patterns obtained are discussed. Additional peaks can be observed i.e. (111), (222), (422), (533). These peaks are attributed to the hematite phase which consists of unreacted Fe_2O_3. This may be due to the reaction not being fully completed or the stopping of the reaction prematurely. Studies showed that at more than 15% loading of CNTs , a well distinct peak appears at $2\theta = 26.0^o$ [33]which is the characteristic peak (0 0 2) corresponding to the graphitic reflection of MWCNTs. The (002) peak is not visible in our graphs as the loading of the MWCNTs was less than the critical loading, any relatively small peaks are also missing. This can be attributed to complete decoration of the MWCNTs with the ferrite nanoparticles. Also with the increased concentration of MWCNTs, the intensity of the peak (311) is relatively decreasing, showing decrease in crystallinity, owing to the formation of more and more defects with the increasing concentration of MWCNTs. The average crystallite size for each XRD pattern was computed for the most intense peak (311) using the Debye's Scherer formula.

The average crystallite size was found to be in the range of 22 nm to 56 nm indicating the formation of small grain sizes. The porosity fraction was calculated using equation 3.6

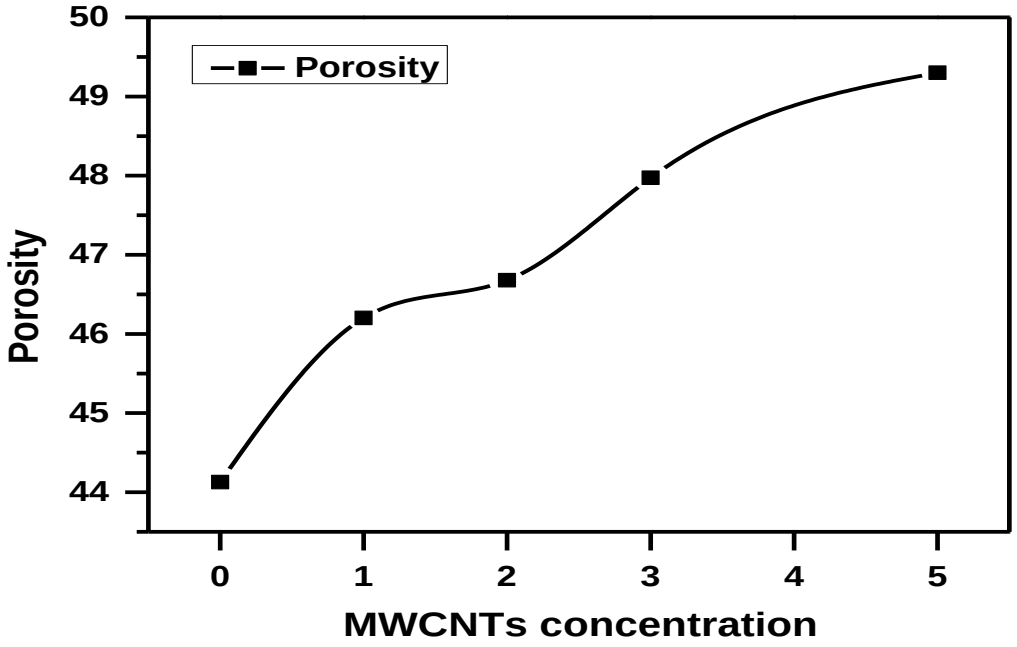

Fig 4.2: Porosity Fraction as a function of increasing concentration of MWCNTs

The porosity fraction also shows a general increasing trend with, with a decreasing rate, while increasing MWCNTs loading[34] owing to the weightless mass and considerably porous MWCNTs, further authenticating the homogenization of ferrite/MWCNTs nano hybrid. Furthermore, with more and more loading of MWCNTs, the quantity of interfaces between ferrite and nanotubes is increasing, which means that there will be more defects within the grains, which also increases the porosity. Parameters including lattice constant, volume of the unit cell, bulk density, X-ray density etc are shown in the following tables:

Table 4.1 XRD stats for the prepared samples

MWCNTs Concentration	X-Ray density (g/cm^3)	Molecular density (g/cm^3)	Porosity (%)
0%	5.277	2.948	44.13
1%	5.225	2.811	46.20
2%	5.184	2.764	46.68

3%	5.058	2.631	47.97
5%	4.989	2.530	49.30

The plots for bulk density and X-ray density for respective MWCNTs concentrations are shown below.

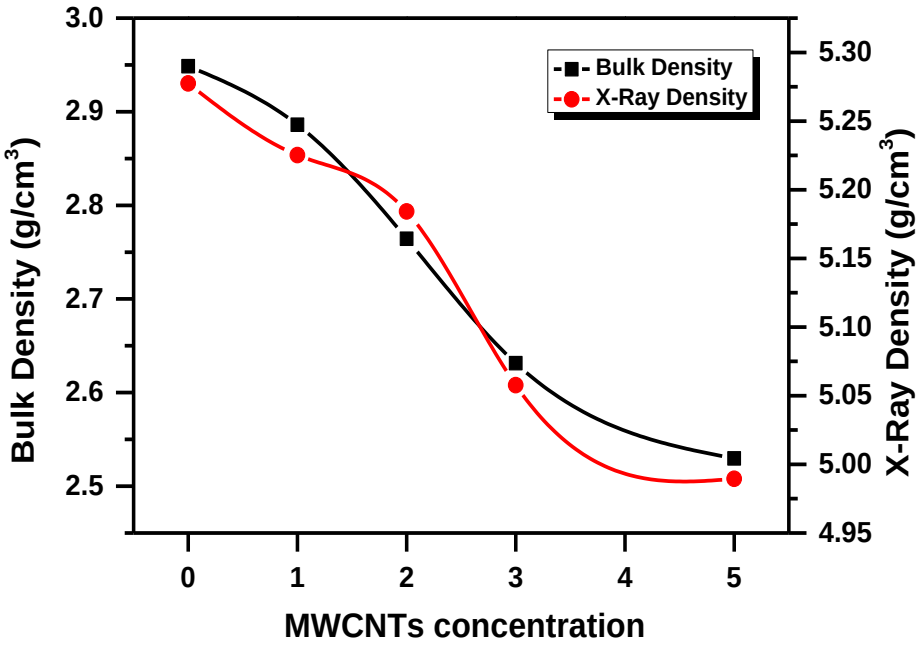

Fig 4.3: Bulk and X- Ray Density as a function of increasing concentration of MWCNTs

The bulk density is the ratio of mass of a solid to its total volume (including solid volume, volume of defects and volume of pores). MWCNTs, being porous, increase the overall porous volume, without adding substantial mass, resulting in a decrease in the bulk density as shown in the above graph.

X-ray density is the ratio between mass of the unit cell to volume of the unit cell. The MWCNTs have high volume with low mass. The decrease in X-Ray density is predictable as the addition of MWCNTs, which have a considerable volume, increase the overall volume of the composite system without adding much weight to the composite. As the percentage of the MWCNTs is increased the overall density of the system decreases. As more and more percentage by weight of MWCNTs is added the effect on the density leaves the linear relation due to the massive difference in the mass as compared to the volume. This is shown in the above graph.

4.2 SEM Results:

The morphology and size of $Ni_{0.5}Zn_{0.5}Fe_2O_4$ nanoparticles decorated on MWCNTs are discussed using SEM. All the sample results showed the same features. So here only the results of pristine MWCNTs, pure $Ni_{0.5}Zn_{0.5}Fe_2O_4$ and its loading onto a MWCNTs is shown

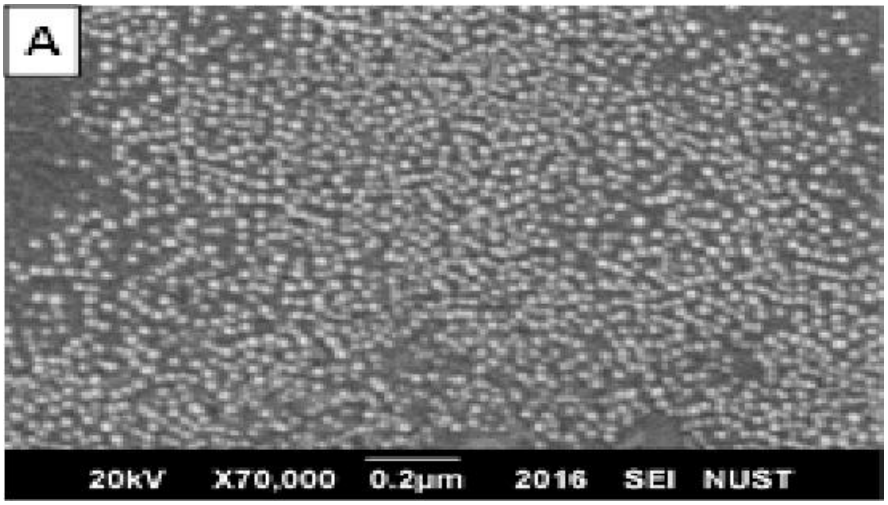

Fig. 4.4 SEM of nano- particles of ferrite

It may be seen that MWCNTs are fully coated with $Ni_{0.5}Zn_{0.5}Fe_2O_4$ nanoparticles confirming that our dispersion procedure for manufacturing of the nano composite is efficient. The particles are homogeneously distributed and aligned along the surface of MWCNTs[35]. The nanoparticles are of different size, ranging from 25nm to 60nm which compliments the results calculated crystallite size by Scherer formula. The small amount of agglomeration observed is due to the heat treatment leading to diffusion of atoms causing crystallite clusters which have become cemented together. When particles normally come into contact with each other and under favorable energy conditions, some of them grow while others decrease in size and eventually disappears. result is usually a small number of large particles as evident from these SEM images.

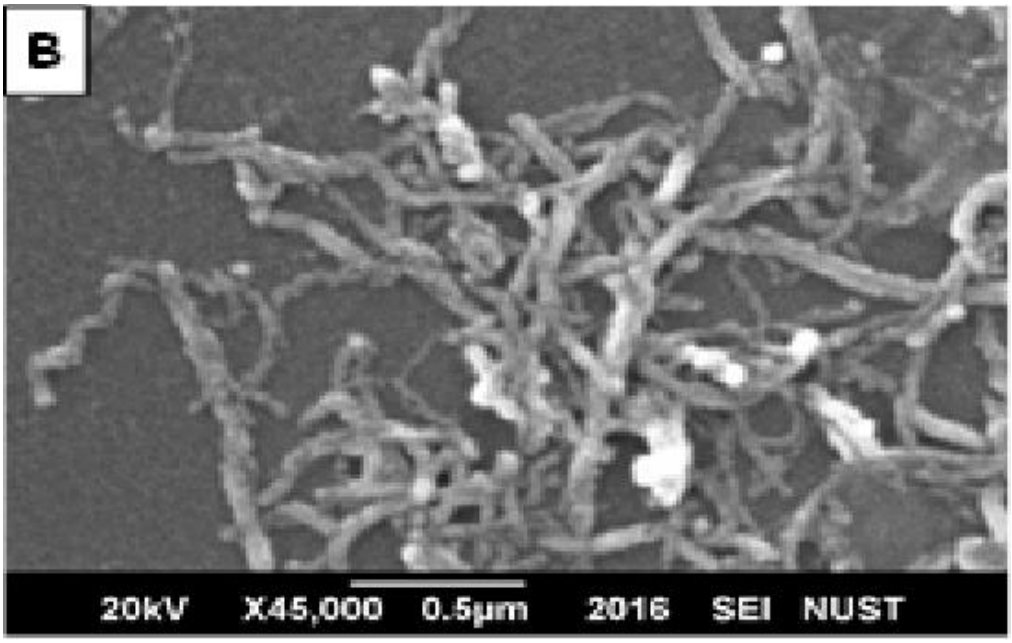

Fig 4.5 SEM of Multiwall Carbon Nanotubes

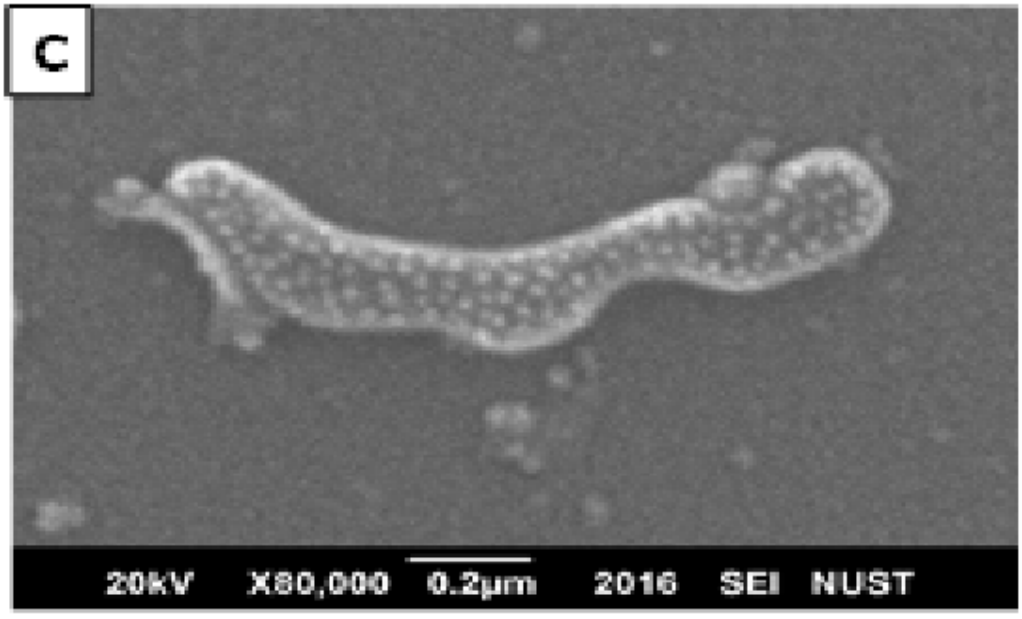

Fig 4.6 SEM of MWCNTs coated/decorated with ferrite particles

4.3 Dielectric/Permittivity Results:

Both dielectric constant E (real part) and dielectric loss factor E" (imaginary part) account for charge storage capacity/polarization ability and energy dissipation.

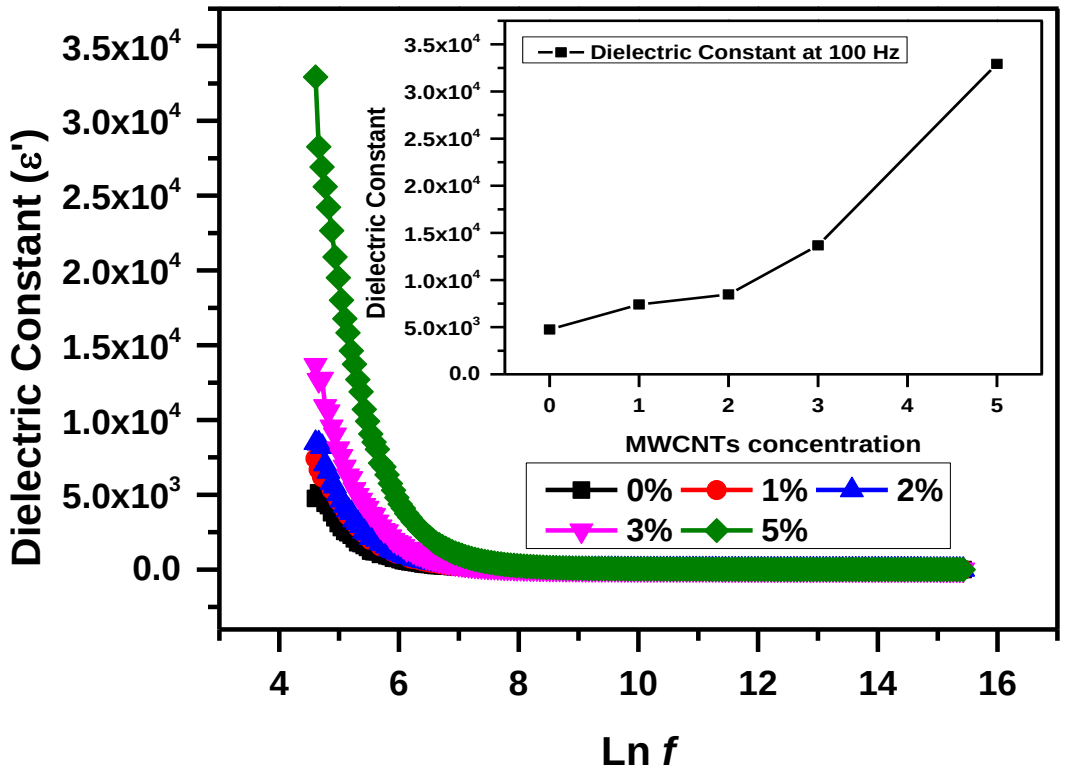

Fig 4.7: Dielectric constant as a function of frequency and Dielectric constant at 100 Hz Frequency

It can be seen that with increased MWCNTs loading, **ε′** increases massively at low frequency. This can be attributed to increased conductivity and high aspect ratio of MWCNTs which are forming conductive network within ferritic matrix. More charge is stored because of the high surface area of the MWCNTs. The maximum values were observed for $Ni_{0.5}Zn_{0.5}Fe_2O_4$ with maximum loading of MWCNTs [36]. In general, the dielectric constant has high values at low values of frequency which decreases gradually

with increasing frequency. This may be explained by MWCNTs conducting network acting as parallel plate capacitors, the polarization effect between which enhances the capacity for storing charges[37]. While at higher frequency range, the dipoles cannot position themselves fast enough and keep up with the applied field; hence, decreasing the dielectric constant, as frequency increases. The dielectric loss factor also shows a similar pattern with increasing frequency as shown in the figure below.

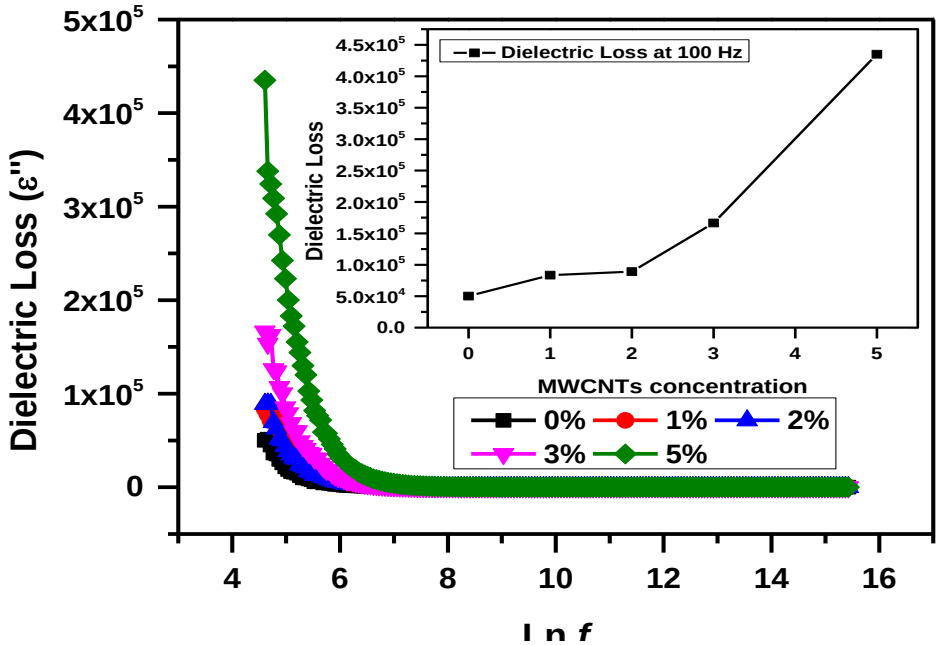

Fig 4.8: Dielectric Loss Factor as a function of frequency and Dielectric Loss Factor at 100Hz frequency

The higher values of dielectric loss factor is due to π bonds, high specific surface area and amplified number of voids and interfaces forming between MWCNTs and ferrite nanoparticles offering high resistance path[6, 37]. The structure causes ease of space charge polarization formation resulting in high dielectric loss values. However, the space charge polarization decreases with high frequency, causing a decrease in loss factor with increasing frequency. The tangent loss factor, which is the ratio of dielectric loss factor to dielectric constant, is shown with increasing frequency for the respective MWCNTs concentrations as below. It is evident that the hybrid with low concentrations of MWCNTs is suitable for dielectric applications.

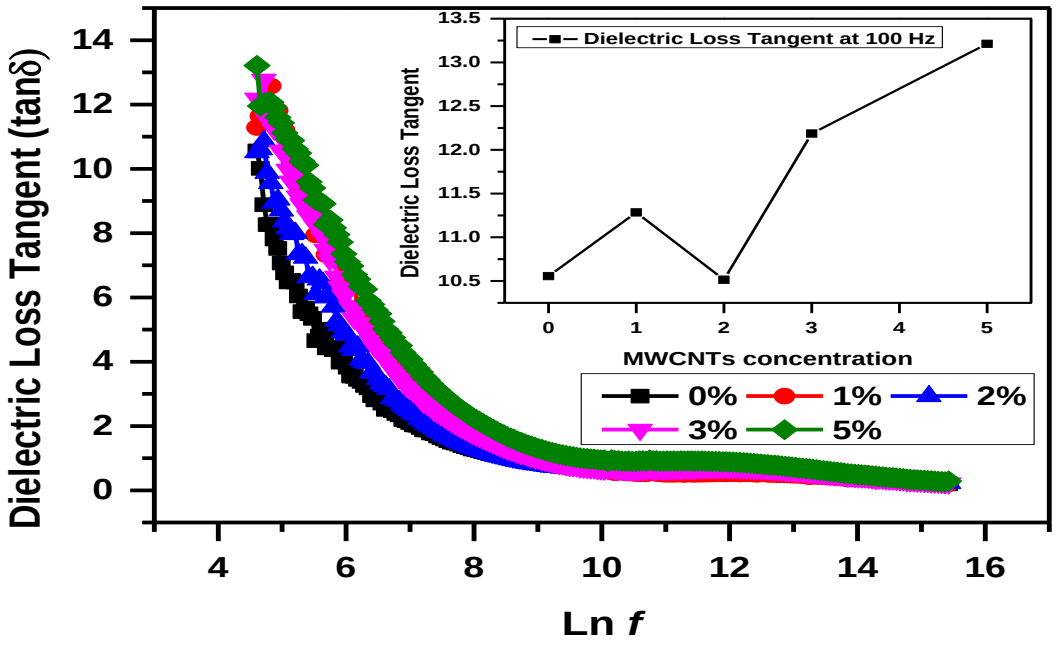

Fig 4.9: Tangent Loss Factor as a function of frequency

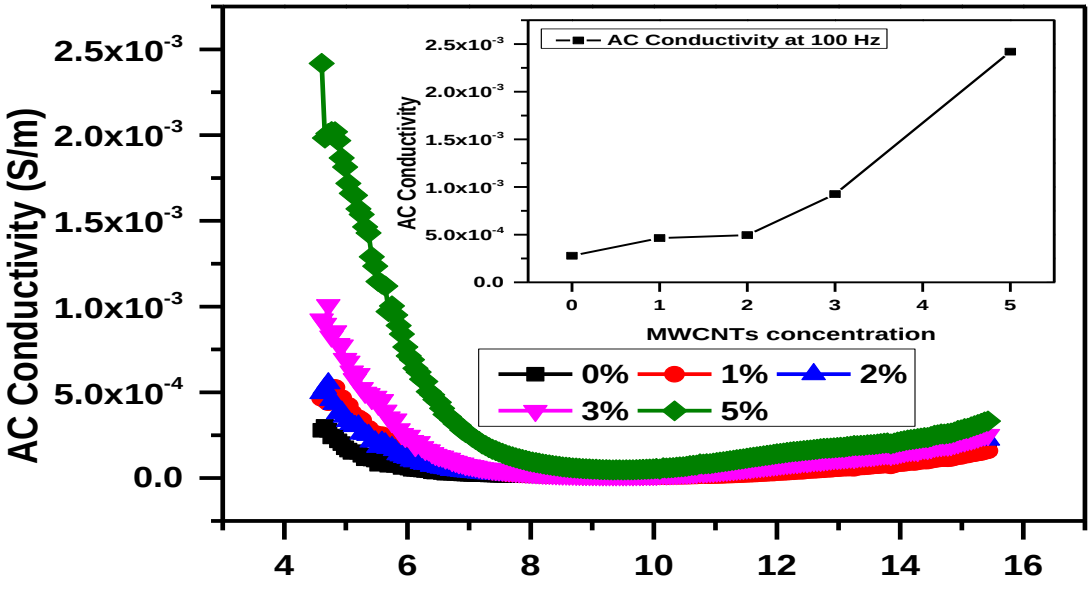

Fig 4.10: AC-Conductivity as a function of frequency and AC- Conductivity at 100 Hz

The picture displayed on the previous page shows a typical AC-Conductivity behavior for the prepared nano- hybrid. Increasing the concentration of MWCNTs from 0% to 5% enhances the overall values of AC- conductivity [38], the highest value may be seen at the most loading i.e. 2.42 x 10^{-3} at a loading of 5%. Increasing the frequency causes the AC- conductivity to decrease as the electrons keep changing direction and are not transmitted. Furthermore, the prevailing hopping mechanism which becomes more likely as the frequency increases hinders with the conductive framework and AC-Conductivity decreases with increasing frequency due to band conduction domination. Ferritic behavior is dominating as the AC-Conductivity increases with increasing frequency owing to the domination of hopping conduction of electrons.

Conclusion:

In the present work, Nickel- Zinc nano- ferrite ($Ni_{0.5}Zn_{0.5}Fe_2O_4$) particles were decorated on MWCNTs using a simple yet effective dispersion route with ortho-xylene as a solvent. The nanoparticles were created using co-precipitation method, resulting in a favorable size range of the crystals. The X-ray powder diffraction technique was used to determine the phase formation. The obtained XRD pattern confirmed the formation of face centered cubic close pack arrangement of nanoparticles. Additional peaks observed confirmed the reaction should be allowed to carry on a little more. The crystallite size, calculated using the Scherer formula, was in the range of 22 nm to 56 nm showing the formation of small grains. With the increase in the MWCNT loading caused the bulk density and the X-Ray density to decrease. The increase in porosity fraction was as expected due to the huge gain in volume as of the MWCNTs and their relatively negligible mass. The SEM images confirmed the formation of nanoparticles and the fixing of these particles to the MWCNTs. The agglomerates were also observed were caused because of the heat treatment (calcination) process causing diffusion of the atoms and the formation of agglomerates. The particles sizes found in SEM images were in complete agreement with the results of XRD. The dielectric properties were massively enhanced due to the high surface area of MWCNTs which formed a conducting framework with the ferrites. The dielectric loss factor also increased, showing that small values of MWCNT addition would be ideal for high dielectric values with minimal loss factor. The AC conductivity showed a dominating trend of ferrite as well as MWCNT's nature. At higher concentrations of MWCNTs, the conducting framework guides the flow of electrons to the background; while at low concentrations, the hopping mechanism dominates resulting in hopping mechanism conduction. As a conclusion, the AC-conductivity improved with the addition of MWCNTs. The experimental route proved to be an efficient, inexpensive and straight forward procedure for the synthesis of ferrite/MWCNTs nano- hybrid and may be considered reproducible.

Future Work:

Such a nano- hybrid can absorb electromagnetic spectrum, so the studies of their Microwave absorption as well as UV-Vis and Infra-red characterization can provide us with data which may be used in various application including but not exclusive to the military. To add conductivity to polymer blends, metallic media is introduced using various polymerization techniques. It would be a natural step to add such a nano- hybrid in a polymer matrix to study the mechanical, electrical and the microwave properties of such an advanced hybrid. Owing to their enhanced dielectric properties, such a nano-hybrid may be used in batteries as a cathode material along with use in the construction of aerospace parts by mixing it with thermoset resins allowing them properties of high stiffness and strength even at very high temperatures. The field of composites has advanced considerably with many different mixes being used in many different industries, a hybrid such as mentioned above can revolutionize the field of nanoscience as well as nanotechnology, creating new boundaries in the realm of magnetism, dielectric, optical and electromagnetic application.

References:

1. Mathew, D.S. and R.-S. Juang, *An overview of the structure and magnetism of spinel ferrite nanoparticles and their synthesis in microemulsions.* Chemical Engineering Journal, 2007. **129**(1-3): p. 51-65.
2. Rahman, O.u., S.C. Mohapatra, and S. Ahmad, *Fe3O4 inverse spinal super paramagnetic nanoparticles.* Materials Chemistry and Physics, 2012. **132**(1): p. 196-202.
3. Ederer, C. and N.A. Spaldin, *Weak ferromagnetism and magnetoelectric coupling in bismuth ferrite.* Physical Review B, 2005. **71**(6).
4. Morin, F.J., *Oxides Which Show a Metal-to-Insulator Transition at the Neel Temperature.* Physical Review Letters, 1959. **3**(1): p. 34-36.
5. Bedanta, S. and W. Kleemann, *Supermagnetism.* Journal of Physics D: Applied Physics, 2009. **42**(1): p. 013001.
6. Hong, X., et al., *A novel ternary hybrid electromagnetic wave-absorbing composite based on BaFe11.92(LaNd)0.04O19-titanium dioxide/multiwalled carbon nanotubes/polythiophene.* Composites Science and Technology, 2015. **117**: p. 215-224.
7. Popov, V., *Carbon nanotubes: properties and application.* Materials Science and Engineering: R: Reports, 2004. **43**(3): p. 61-102.
8. Zhao, D.-L., et al., *Electromagnetic and microwave absorbing properties of Co-filled carbon nanotubes.* Journal of Alloys and Compounds, 2010. **505**(2): p. 712-716.
9. Bai, Y., et al., *High-dielectric-constant ceramic-powder polymer composites.* Applied Physics Letters, 2000. **76**(25): p. 3804.
10. Li, J., et al., *Bottom-up versus top-down effects on ciliate community composition in four eutrophic lakes (China).* European Journal of Protistology, 2016. **53**: p. 20-30.
11. Simon, P. and Y. Gogotsi, *Materials for electrochemical capacitors.* Nat Mater, 2008. **7**(11): p. 845-854.
12. Yoon, T.J., et al., *Multifunctional nanoparticles possessing a "magnetic motor effect" for drug or gene delivery.* Angew Chem Int Ed Engl, 2005. **44**(7): p. 1068-71.
13. Hung, K., et al., *Wide-temperature range operation supercapacitors from nanostructured activated carbon fabric.* Journal of Power Sources, 2009. **193**(2): p. 944-949.
14. Yu, G., et al., *Hybrid nanostructured materials for high-performance electrochemical capacitors.* Nano Energy, 2013. **2**(2): p. 213-234.
15. Ghasemi, A., *The role of multi-walled carbon nanotubes on the magnetic and reflection loss characteristics of substituted strontium ferrite nanoparticles.* Journal of Magnetism and Magnetic Materials, 2013. **330**: p. 163-168.

16. Verma, A., A.K. Saxena, and D.C. Dube, *Microwave permittivity and permeability of ferrite–polymer thick films.* Journal of Magnetism and Magnetic Materials, 2003. **263**(1-2): p. 228-234.
17. Hussain, S.T., et al., *Decoration of carbon nanotubes with magnetic Ni1−xCoxFe2O4 nanoparticles by microemulsion method.* Journal of Alloys and Compounds, 2012. **544**: p. 99-104.
18. Abdel Salam, M., M.A. Gabal, and A.Y. Obaid, *Preparation and characterization of magnetic multi-walled carbon nanotubes/ferrite nanocomposite and its application for the removal of aniline from aqueous solution.* Synthetic Metals, 2012. **161**(23-24): p. 2651-2658.
19. Murugesan, C., M. Perumal, and G. Chandrasekaran, *Structural, dielectric and magnetic properties of nickel zinc ferrite prepared using auto combustion and ceramic route.* Physica B: Condensed Matter, 2014. **448**: p. 53-56.
20. Sajjia, M., et al., *Developments of nickel zinc ferrite nanoparticles prepared by the sol–gel process.* Ceramics International, 2014. **40**(1): p. 1147-1154.
21. Wu, H., et al., *Solvothermal synthesis of nickel zinc ferrite nanoparticles loaded on multiwalled carbon nanotubes for magnetic resonance imaging and drug delivery.* Acta Biomaterialia, 2011. **7**(9): p. 3496-3504.
22. Nikumbh, A.K., et al., *Structural, electrical, magnetic and dielectric properties of rare-earth substituted nickel zinc ferrites nanoparticles synthesized by the co-precipitation method.* Journal of Magnetism and Magnetic Materials, 2014. **355**: p. 201-209.
23. Melo, R.S., et al., *Magnetic ferrites synthesised using the microwave-hydrothermal method.* Journal of Magnetism and Magnetic Materials, 2015. **381**: p. 109-115.
24. Güven Özdemir, Z., et al., *Super-capacitive behavior of carbon nano tube doped 11-(4-cyanobiphenyl-4-oxy) undecan-1-ol.* Journal of Molecular Liquids, 2015. **211**: p. 442-447.
25. Ali, A.A., et al., *MWCNTs/carbon nano fibril composite papers for fuel cell and super capacitor applications.* Journal of Electrostatics, 2015. **73**: p. 12-18.
26. Kumar, R., et al., *Graphene-wrapped and nickel zinc oxide-intercalated hybrid for extremely durable super-capacitor with ultrahigh energy and power densities.* Carbon, 2014. **79**: p. 192-202.
27. Liu, Y., et al., *EMI shielding performance of nanocomposites with MWCNTs, nanosized Fe3O4 and Fe.* Composites Part B: Engineering, 2014. **63**: p. 34-40.
28. Gul, I.H., et al., *Structural, magnetic and electrical properties of Co1−xZnxFe2O4 synthesized by co-precipitation method.* Journal of Magnetism and Magnetic Materials, 2007. **311**(2): p. 494-499.
29. Zhang, Y., et al., *Composition and magnetic properties of nickel zinc ferrite nano-particles prepared by the co-precipitation method.* Journal of Magnetism and Magnetic Materials, 2010. **322**(21): p. 3470-3475.
30. Xie, H., et al., *An improved continuous co-precipitation method to synthesize LiNi0.80Co0.15Al0.05O2 cathode material.* Journal of Alloys and Compounds, 2016. **666**: p. 84-87.

31. Zhang, Q., et al., *Synthesis and characterization of carbon nanotubes decorated with manganese–zinc ferrite nanospheres.* Materials Chemistry and Physics, 2009. **116**(2-3): p. 658-662.
32. Sutradhar, S., S. Das, and P.K. Chakrabarti, *Magnetic and enhanced microwave absorption properties of nanoparticles of Li0.32Zn0.26Cu0.1Fe2.32O4 encapsulated in carbon nanotubes.* Materials Letters, 2013. **95**: p. 145-148.
33. Zhou, X., et al., *Microwave sintering carbon nanotube/Ni0.5Zn0.5Fe2O4 composites and their electromagnetic performance.* Journal of the European Ceramic Society, 2013. **33**(11): p. 2119-2126.
34. <*1393_Hakeem.pdf*>.
35. Asghari, M., et al., *Evaluation of microwave and magnetic properties of substituted SrFe12O19 and substituted SrFe12O19/multi-walled carbon nanotubes nanocomposites.* Materials Chemistry and Physics, 2013. **143**(1): p. 161-166.
36. Tyagi, S., et al., *Microwave absorption study of carbon nano tubes dispersed hard/soft ferrite nanocomposite.* Ceramics International, 2012. **38**(6): p. 4561-4571.
37. Zhou, X.-B., et al., *Preparation of nanocrystalline-coated carbon nanotube/Ni0.5Zn0.5Fe2O4composite with excellent electromagnetic property as microwave absorber.* Journal of Physics D: Applied Physics, 2013. **46**(14): p. 145002.
38. Unal, B., et al., *Multiwall-carbon nanotube/nickel zinc ferrite hybrid: Synthesis, magnetic and conductivity characterization.* Current Applied Physics, 2013. **13**(7): p. 1404-1412.